THE UNIVERSITY OF CALGARY

Dynamic Simulation of a Reciprocating Compressor During an Emergency Shut Down

by

James K. Beckie

A THESIS SUBMITTED TO THE FACULTY OF GRADUATE STUDIES

IN PARTIAL FULFILLMENT OF THE REQUIREMENTS FOR THE

DEGREE OF

MASTER of ENGINEERING

DEPARTMENT OF

CHEMICAL and PETROLEUM ENGINEERING

CALGARY ALBERTA

JUNE 1988

ISBN 0-315-46552-2

THE UNIVERSITY OF CALGARY

FACULTY OF GRADUATE STUDIES

The undersigned certify that they have read, and recommend to the Faculty of Graduate Studies for acceptance, a thesis entitled,

"DYNAMIC SIMULATION OF A RECIPROCATING COMPRESSOR DURING AN EMERGENCY SHUT DOWN"

submitted by James Kenneth Beckie in partial fulfillment of the requirements for the degree of Master of Engineering.

W. Svrcek

Dr. W.Y. Svrcek, Committee Chairman
Dept. of Chemical & Petroleum Engineering

R. J. Moore

Dr. R.G. Moore
Dept. of Chemical & Petroleum Engineering

Mark Trebble

Dr. M. Trebble
Dept. of Chemical & Petroleum Engineering

J. A. C. Kentfield

Dr. J. Kentfield
Dept. of Mechanical Engineering

R. Estep

Mr. R. Estep, Dome Petroleum
External Examiner

June 23, 1988

Date

ABSTRACT

A model was developed to simulate the system response of a reciprocating compressor during an emergency shut down. The dynamics of the depressuring sequence are a function of the design of the compressor facility. All of the components of the facility were integrated into one model. From the model a computer program was written for a personal computer. The program has the flexibility to quantify the effect that different design philosophies have on the dynamics of the depressuring sequence.

It is important to accurately predict the pressure transients to prevent the system from exceeding the design pressure during an emergency compressor shut down. The installation of additional flare valves and the action of the valves during an emergency shut down were investigated to determine the system response. System response is also affected by the size of the system and the pressure of the gas contained within the system. The model was verified by matching the predictions to the measured data from three industrial compressors, of different sizes and operating pressures. The model successfuly predicted both the dynamic response to changes in system configuration and the compressor run down time.

ACKNOWLEDGMENTS

The author wishes to express his gratitude to Dr. W.Y. Svrcek for the guidance and support that made this project possible. Special thanks are also extended to Rob Estep and Wayne Sim who were always willing to offer their valuable ideas and assistance.

I am also particularly grateful to Mr. Ray Babiuk and Mr. Wade Patten of Dome Petroleum for their invaluable assistance in obtaining industrial data.

Finally I am grateful to Darcy Beckie for her support and editing skills.

Table of Contents

List of Tables

List of Figures

NOMENCLATURE

VARIABLES

b_1, b_2, b_3, b_4 - Lee Kesler constants (Table 5.1)

clearance - clearance at end of cylinder

C_g - Fisher valve flow characteristic

C_1 - Fisher valve constant

c_1, c_2, c_3, c_4 - Lee Kesler constants (Table 5.1)

Cp - isobaric heat capacity

Cv - isochoric heat capacity

d_1, d_2 - Lee Kesler constants (Table 5.1)

D - diameter

E - intermediate value as defined by equation 5.8

f - friction factor

FloMAX - maximum compressor flowrate

g - gas gravity

g_c - gravitational constant

h - losthead

I - Inertia

K - Heat capacity ratio (Cp/Cv)

MaxRPM - Maximum RPM

MW - Molecular Weight

n - number of moles

$\dot{n}$ - molar flowrate

P	-Pressure
Position	-Valve position (0-100%)
Q	-flowrate
Re	-Reynolds*number*
R	-ideal gas constant
R_2	-connecting rod length (Figure 4.1)
R_3	-crank lobe length (Figure 4.1)
RPM	-rotational speed (revolutions/minute)
S_o	-area of orifice
T	-Temperature
V	-Volume
Vel	-velocity
x	-mole fraction
X_B	-piston displacement (Figure 4.1)
Y_o	-orifice constant
Z	-Compressibility Factor

SUBSCRIPTS

c	-critical
CE	-crankend
cm	-mixture critical
compflo	-flowrate at time t through the compressor station
cyl	-cylinder
d	-downstream
disflarflo	-flow from the discharge flare valve

flar	-flare
flarflo	-flow from the flare valve
floESDV	-flow from the ESDV valve
HE	-head end
i	-component i
j	-component j
k	-component k
o	-orifice plate
p	-pipe
pist	-piston
r	-reduced property
recflo	-flow from the recycle valve
rod	-piston rod
sc	-standard condition (101.325 kPa, 15°C)
sucflarflo	-flow from the suction flare valve
t	-time
u	-upstream

SUPERSCRIPTS

H°	-ideal enthalpy

GREEK LETTERS

β	- ratio of orifice to pipe diameter and constant in table 5.1
γ	-constant defined in table 5.1
Δ	-change in variable
ϵ	-intermediate viscosity variable
θ	-crankangle
μ	-viscosity
π	-3.1415
ρ	-density
τ	-torque
ω	-rotational speed or thermodynamic acentric factor

CHAPTER 1

PROJECT DEFINITION

1.1 INTRODUCTION

Reciprocating compressors are used in a large number of applications in the oil and gas industry. Reciprocating compressor installations require sophisticated control systems to protect the facility during start up and operation. When the compressor is incorrectly shut down the dynamic behavior of the system can result in damage to the compressor and associated equipment. Specifically, the pressure in the associated piping can exceed design pressures unless the shut down logic incorporates a prediction of the pressure transients during depressurization.

It is of utmost importance that the block depressuring and flare system be designed to depressure the compressor safely in the event of an emergency. The cost of upgrading the system to absorb any potential hazards is much more expensive than designing the system properly. The design engineer must develop a design that incorporates both rapid depressuring of the compressor and a properly sized flare system.

The objective of this thesis is to develop a model to predict transient pressures and flowrates in this type of facility during the depressuring of the compressor.

1.2 PROJECT RATIONALE

The design of the safety system must ensure that the dynamics of starting, operating and shutting down the compressor do not lead to a hazardous situation. Hazardous situations may arise from: vibration, gas leaks, fire, and overpressuring of piping and vessels.

The compressor and associated piping are protected from overpressuring by two independent safety systems, the high pressure shut down and the automatic pressure safety relief valves. The high pressure shut down is activated when the system pressure exceeds the high setpoint pressure. The control panel high pressure shut down is set at 90 to 95 % of the maximum operating pressure of the vessel. If the high pressure shut down does not operate, the Pressure Safety Valves (PSVs) will depressure the system to maintain the measured pressure at or below the maximum operating pressure of the vessel. The PSV has to be sized to relieve the maximum flowrate required to maintain the system below it's maximum operating pressure.

Difficulties often arise in determining the maximum flowrate during the depressuring procedure. The dynamics of the shut down sequence depend on the system configuration. To date there has been no easy way to formulate a rigorous model describing the dynamics of the entire system. At present a great many assumptions are made to simplify the system for preliminary predictions. These assumptions tend to oversimplify the system and overlook the instantaneous pressures and flowrates that can exceed the design specifications of the facility.

1.3 PROJECT SCOPE

The scope of this project was to investigate the compressor shut down phenomenon and to simulate this behavior with a computer program. To this end the depressuring sequence was broken down into a number of areas of investigation as outlined in section 1.3.1. Each of the areas of investigation were integrated into one model so that when one component is altered the effect on the entire system can be predicted.

To verify the model's reliability the predictions were compared to the actual shut down data recorded for the following compressors:

1) The Reinjection Compressor #2 located at Dome's West Pembina Gas Plant. Data recorded in June 1987.

2) The Brazeau Cardium Compressors located in Dome's West Pembina Field. Data recorded in April 1988.

3) The Reinjection Compressor #1 located at Dome's West Pembina Gas Plant.

These compressors were chosen to demonstrate the model's ability to predict the depressuring data from two very different compressor installations. The Reinjection Compressor #2 is a 2600 kW compressor discharging at 35,000 kPa abs and a flowrate of 730 $10^3 m^3_{sc}$/day. The Cardium facility is comprised of two parallel 370 kW compressors discharging at 3000 kPa abs and a total flowrate of 200 $10^3 m^3_{sc}$/day.

1.3.1 AREAS OF INVESTIGATION

The following areas of investigation were integrated into one comprehensive model as shown in Figure 1.1.

1) Transient Piping Pressures - predicted the instantaneous pressures during the entire depressuring sequence.

2) Flare System - predicted the flowrates, temperatures and pressures during the shut down sequence.

3) Depressuring Time - calculated the time it takes to depressure the entire system to a predetermined safe endpoint pressure.

4) Compressor Rundown Time - predicted the time for the compressor to stop rotating when the power is removed from the driver.

5) Recycle Valve - investigated the effect of the recycle valve fail position on the pipe pressures.

6) Flare Valves - investigated the need to install a flare valve on the suction line and determine the optimum size of the flare valve.

7) Emergency Shut Down Block Valves - predicted the time to close the automatic suction and discharge block valves.

8) Thermodynamics Property Package - developed to facilitate the prediction of pressures and temperatures.

1.4 PROGRAM DEVELOPMENT

The program was developed using Borland's Turbo Pascal Software[1] on a WYSE personal computer 286. The ratio of Central Processing Unit (CPU) time to real time was 1.8 for the Cardium Compressors and .35 for the Reinjection Compressors #1 and #2. The higher ratio for the Cardium Compressors was the result of a very short depressuring time of 1 minute versus the Reinjection Compressor #2 depressuring time of 25 minutes. This implies that the Cardium Compressor required more calculations per time step than for Reinjection Compressor #2.

FIGURE 1.1

PROGRAM FLOWSHEET TO CALCULATE COMPRESSOR BLOWDOWN TIME DURING AN EMERGENCY SHUTDOWN OF A COMPRESSOR STATION

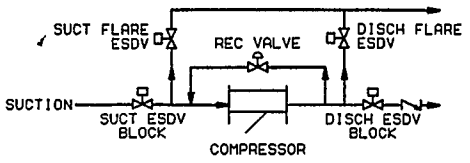

ESD - EMERGENCY SHUTDOWN
ESDV - EMERGENCY SHUTDOWN VALVE

NOTE:

1. COMPRESSOR RUNNING WHICH COMPRESSES GAS FROM SUCTION TO DISCHARGE AND AFFECTS:
   A) SUCTION PRESSURE DECREASES AND MAY CAUSE RAREFACTION.
   B) DISCHARGE PRESSURE INCREASE AND MAY CAUSE OVERPRESSURE.
2. PRESSURES IN SUCTION & DISCHARGE AFFECT THE COMPRESSOR RUN DOWN TIME.
3. ACTUATOR TRAVEL RATE IS LIMITED BY SOLONID.

CHAPTER 2

COMPRESSOR SAFETY EQUIPMENT

Since compressor facilities represent a large investment it is important that a safety system be in place. Protection of these facilities is accomplished by a network of safety features. The environment within the building is monitored by fire and gas detectors. The operating conditions of the compressor are monitored by a local control panel and by the plant operators in the control room. If the fire detector, gas detector, control panel or an operator detect an emergency situation the emergency shut down sequence is activated. Upon an emergency signal the compressor facility will immediately block all suction and discharge piping and depressure the system to flare. The compressor shut down logic dictates the sequence of events upon an emergency shut down signal. Automatic safety valves provide the mechanism to block and depressure the facility.

2.1 COMPRESSOR SHUT DOWN LOGIC

Two distinct levels of shut down logic protect the compressor. The first level is designed to provide mechanical protection for the compressor and driver. The second level is set up to protect the building and equipment from major damage. In addition to protecting equipment each

system enables operators to identify equipment problems by a first-out annunciator system. The first-out annunciator system leaves a flag on the control panel to indicate the cause of the shut down.

The first level of the compressor shut down logic is pre-programmed into the local control panel instruments. The control panel instrumentation senses the compressor operating data and compares the data to high setpoint values. The high setpoint values are designed to protect the compressor against the following:

1) High Discharge Temperature - protection of non-metallic compressor parts and lubricants.

2) High Discharge Pressure - protection against overloading the piston rods and overpressuring piping.

3) Low Suction Pressure - protection against overloading the piston rods.

4) Low Discharge Pressure - protection in the event of a discharge pipe break.

5) Lubrication - protection in the event of insufficient lubricant.

6) Cooling Fluid Circulation - protection against inadequate circulation of cooling fluids.

7) Electric Driver Purge Air - protects the electric driver if the purge air system fails to supply sufficient air flow.

The second level of shut down activates the emergency shut down block and depressure sequence if any of the following alarm conditions are activated:

1) High Gas Alarm - gas sensors set at 40% of lower explosion limit.
2) Fire Detection - ultraviolet sensors detect open flame.
3) Instrument Air Failure - air pressure drops below low setpoint pressure because the instrumentation is air operated.
4) Backup Power Failure - backup power drops below low setpoint voltage.
5) Manual Emergency Shut Down (ESD) - switch activated by operator from control panel or building wall.

Each time the compressor blocks and depressures the operator must re-pressure the compressor prior to start up. The reinjection compressors at West Pembina are all designed to block and depressure on the five shut downs listed above plus on any control panel or switchgear related shut down. This is a necessary precaution for reinjection compressors due to their high discharge pressures. The high pressure discharge gas must be depressured while hot because if the

gas is allowed to cool to ambient temperature, the gas being throttled through the flare valve would decrease to a cryogenic temperature.

The safety of the compressor is ensured by incorporating the specific shut down logic in the local control panel, the switchgear and the main control panel. The shut down logic is designed to regulate the system in the event of an emergency depressuring. The shut down logic includes the consideration of the opening or closing of each automatic valve. In addition the sequence of valve action must be preset for every shut down condition.

2.2 AUTOMATIC VALVES

Automatic valves are located at strategic positions to block and depressure the compressor and associated piping. In Figure 2.1 a typical two stage compressor and emergency depressuring system is shown. Gas is compressed from suction to discharge and cooled at each stage with an intercooler and aftercooler respectively.

The suction Emergency Shut Down Valve (ESDV) is an automatic block valve located upstream of the compressor to block off the inlet piping. Similarly there is a discharge ESDV

located on the discharge piping. The prime consideration is to close these valves rapidly in an emergency. This function is often overlooked in the overall design. Often the smallest and slowest ESDV closing mechanism is chosen on the basis of cost. The cost of this component is a small percentage of the total facility cost. Hence, at a small additional cost the depressuring time for the compressor can be shortened significantly.

Automatic flare valves are typically placed on the discharge piping because it contains the highest pressure gas. The suction piping is depressured via the compressor. Careful consideration is required when installing a flare valve on the suction piping. The advantage of depressuring the system more rapidly through the suction flare valve, may be outweighed by the risk of drawing air in from the flare stack through the suction flare valve. In addition the flare line would have to be sized larger to accommodate the higher peak flare flowrates as the result of installing a suction flare valve.

TYPICAL 2 STAGE COMPRESSOR FLOW SCHEMATIC

FIGURE 2.1

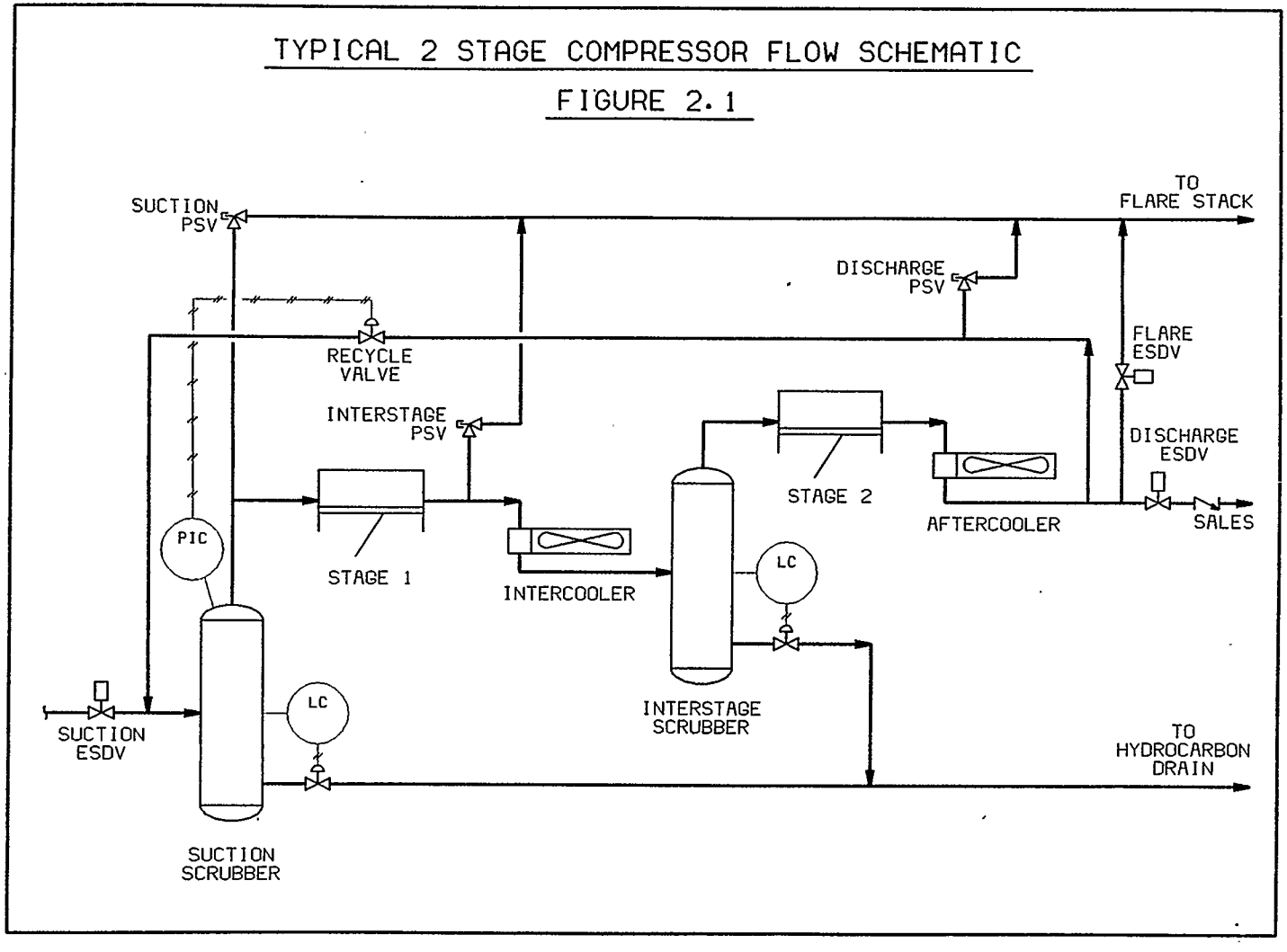

The alternative of only installing the flare valve on the discharge piping results in less than 200 kPa abs residual pressure in the suction piping. The residual pressure is the result of the compressor valves which act as check valves to allow unidirectional flow through the compressor. These check valves are spring loaded valves that require a differential pressure to be unseated. Therefore a residual pressure is left in the suction piping.

It is important to depressure the piping rapidly to prevent the pipe from failing due to overpressuring during a fire. The pressure that is considered safe ranges from 150 to 450 kPa abs depending on the design pressure of the system.

The automatic recycle valve is a multi function valve; it maintains positive pressure on the suction piping, assists in flow control and enables the discharge gas to be recycled to suction for start up. After start up the recycle valve will only open if the suction pressure drops below the low setpoint. Some designers incorrectly believe that the compressor may be depressured more rapidly if the recycle valve is opened during the depressuring sequence. This is a dangerous procedure because if there isn't a flare valve on the suction line the opening of the recycle valve will cause overpressuring of the suction piping. The only consequence

of failing to open the recycle valve is the transfer of gas volume from the discharge piping to the suction piping. Assuming there is no suction flare valve, this transferred volume of gas has to eventually flow back through the compressor to the discharge piping to be depressured through the discharge flare valve.

The PSVs are designed to maintain system pressure at or below the maximum design pressure (m.o.p.) of the piping. The size of the valve is selected for the maximum flowrate required to maintain pressure at or below the m.o.p. of the system. PSV sizing and maintenance are regulated by the government (Boiler's Branch) and engineering standards(API 617 and ASME Section VIII).

CHAPTER 3

COMPRESSOR DEPRESSURING DYNAMICS

The dynamics of compressor depressuring is a function of the pressure and size of the system, the system configuration and the shut down logic. Larger high pressure systems tend to have longer depressuring times. To demonstrate the effect of these variables, three examples from industry are examined. The first two are both high pressure reinjection compressors and are used to illustrate the effect of having different shut down logic. The latter compressor is the Cardium compressor and is used to demonstrate the effect of system size and pressure.

3.1 EXAMPLES FROM INDUSTRY

The dynamics of depressuring is largely a function of the system configuration and the shut down logic. The system configuration determines the initial pressures, the location of valves, and the volumes that will be depressured during the shut down sequence. The shut down logic dictates the valve action and sequence.

The three examples from industry are as follows. The compressors are named Reinjection Compressor #1, Reinjection Compressor #2, and Cardium Compressor. Reinjection Compres-

sor #1 is steam turbine driven unit and was installed in 1983. Reinjection Compressor #2 is driven by an electric motor and was installed in 1987. The Cardium Compressor is also driven by an electric motor and was installed in 1987. All these compressors have identical system configurations as shown in Figure 2.1. Table 3.1 shows the operating conditions for all the compressors.

When the ESD is activated the suction and discharge valves travel to the closed position. The power to the driver and all other utility motors is terminated. When the suction and discharge block valves have closed, the flare valve on the discharge pipe opens. None of the compressors have a suction flare valve due to the concerns outlined in section 2.2.

To demonstrate the effect of different shut down logic, two compressors with identical configurations were studied. Reinjection Compressor #1 and Reinjection Compressor #2 were compared. These compressors operate in parallel at Dome's West Pembina Gas Plant. Each compressor has the same system configuration but historically had different shut down logic. The system configuration on Reinjection #1 has been changed to be identical to Reinjection #2.

When the ESD was activated on Reinjection Compressor #1 the recycle valve failed open and a large volume of gas flowed from the discharge to the suction piping. If the suction pressure was already close to the design limit of the piping, this added volume causes the suction piping pressure to increase rapidly. Because the recycle flow is very high and the PSV was only sized for thermal relief, the suction piping pressure came close to exceeding the maximum design pressure. This problem was a design oversight and was quickly remedied by changing the action of the valve actuator to fail closed.

When the ESD was activated on Reinjection Compressor #2 the recycle valve failed closed. The suction pressure increased slightly because the suction ESDV had not fully closed when the compressor stopped and the feed gas pressure increased as the flow stopped.

To demonstrate the effect of system size and pressure on the predicted results, the Cardium compressor was compared to the results of Reinjection Compressor #2. The Cardium compressor has both smaller throughput and piping volumes. The pressures in the Cardium system are lower than the pressures in Reinjection Compressor #2. The recycle valve

in the Cardium system is designed to remain closed during an ESD and the shut down logic is essentially identical to Reinjection Compressor #2.

Table 3.1

Compressor Operating Conditions

Compressor Characteristics	Reinjection #1 & #2	Cardium
Suction Pressure(kPa abs)	6000.0	325.0
Suction PSV(kPa abs)	10090.0	2150.0
InterStage Pressure(kPa abs)	12000.0	1120.0
Discharge Pressure(kPa abs)	35000.0	3000.0
Discharge S/D Press(kPa abs)	37500.0	4400.0
Discharge PSV (kPa abs)	38011.0	5915.0
Compressor RPM	277.0	900.0
Number of Throws	2.0	2.0
Number of Stages	2.0	2.0
Atmospheric Press(kPa abs)	90.0	90.0
St 1 Suction Temp(C)	15.6	4.4
St 1 Discharge Temp(C)	126.7	100.0
St 2 Suction Temp(C)	48.9	48.9
St 2 Discharge Temp(C)	112.2	65.6
Suction Pipe Volume(m^3)	3.7	0.74
Interstage Pipe Volume(m^3)	2.5	0.59
Discharge Pipe Volume(m^3)	3.0	0.45
System Inertia (kg-m^2)	1016000.0	50000.0
Flare Valve Orifice (mm)	12.5	25.4
Compressor Stroke (mm)	508.0	114.3
Connecting Rod Length(mm)	1270.0	349.3
St 1 Piston Diameter(mm)	247.7	342.9
St 2 Piston Diameter(mm)	161.9	187.3
Rod Diameter (mm)	101.6	50.8
St 1 Head End Clearance (%)	17.1	20.3
St 2 Head End Clearance (%)	14.4	13.2
St 1 Crank End Clearance (%)	15.9	13.9
St 2 Crank End Clearance (%)	19.4	14.4

CHAPTER 4

MODEL DEVELOPMENT

Development of the model was broken down into the areas of investigation as outlined in section 1.3.1 and summarized below. Each area was modeled separately and then integrated into one model.

The mathematical model is composed of the following areas of investigation:

1) Transient Piping Pressures
2) Flare System
3) Depressuring Time
4) Compressor Rundown Time
5) Recycle Valve Fail Position
6) Suction Flare Valves
7) Emergency Shut Down Block Valves

4.1 TRANSIENT PIPING PRESSURE

The transient pressures in the piping are a function of the gas that is flowing between the sections of the compressor and the gas that is flowing to flare. The pressure is calculated at discrete time intervals by completing a mole balance around the region of interest. Assuming the

compressor is compressing only a single phase gas, the pressure is calculated using the Lee Kesler equation of state for compressibility.

4.1.1 Mole Balance

Equations 4.1 and 4.2 are the mole balance equations for the system shown in Figure 2.1 with the additional capability to include a suction flare valve. These equations are derived in Appendix C. The flowrates for the flare, recycle, and suction and discharge block valves are developed in sections 4.1.2 to 4.1.5.

The suction piping mole balance for a small time change is as follows.

$$n_{t+1} = n_t - \left(\dot{n}_{sucflarflo} - \dot{n}_{recflo} - \dot{n}_{floESDV} + \dot{n}_{compflo}\right)\Delta t \qquad -(4.1)$$

The discharge piping mole balance for a small time change is as follows.

$$n_{t+1} = n_t - \left(\dot{n}_{disflarflo} + \dot{n}_{recflo} + \dot{n}_{floESDV.} - \dot{n}_{compflo}\right)\Delta t \qquad -(4.2)$$

4.1.2 Flare Flowrate

Flare flowrate is calculated either from the sonic velocity sizing equations[2] 4.3 to 4.8 or from the Fisher valve sizing equation 4.9[3].

The sonic velocity is calculated as follows:

$$vel_{sonic} = \left\{ \frac{2k}{(k+1)} \frac{ZTR}{MW} \right\}^{0.5} \qquad -(4.3)$$

The orifice velocity is calculated from equations 4.4 to 4.7.

$$S_o = \frac{\pi}{4} D_o^2 \qquad -(4.4)$$

$$\beta_o = \frac{D_o}{D_p} \qquad -(4.5)$$

$$Y_o = 1 - \left\{ .41 + \frac{.35\beta_o^4}{k} \left(1 - \frac{P_d}{P_u} \right) \right\} \qquad -(4.6)$$

$$V_o = .61 Y_o \left\{ 1 - \beta^4 \right\} \sqrt{2 \frac{P_u - P_d}{\rho}} \qquad -(4.7)$$

The values of sonic velocity and orifice velocity are compared and the lower value is selected to use in the calculation of the flare flowrate.

$$\dot{n}_{flarflo} = \text{Position}_{flarvalv} S_o V \left(\frac{P_u}{Z_u T_u} \right) \frac{T_s}{P_s} \qquad -(4.8)$$

Position is a value that is calculated as a percentage of the full open or closed position of the valve. The value of position can vary from 0 to 1.0. The position is calculated in equations 4.37 and 4.38 in section 4.7.

If the valve is a Fisher control valve the Fisher control valve sizing equation for a D body equal percentage valve can be applied.[3]

$$\dot{n}_{flarflo} = \text{Position}_{flarvalv} \sqrt{\frac{298}{gT_u}} C_g P_u \sin\left\{ \frac{3417}{C_1} \sqrt{\left(\frac{P_u - P_d}{P_u} \right)} \right\}_{degrees} \quad -(4.9)$$

4.1.3 Recycle Flowrate

The function of the recycle valve is to control the recirculation of gas from discharge to suction. The recycle valve is used during start up, for flow control and to maintain a preset suction pressure. This valve is generally a control valve and the Fisher valve sizing equation for a D body equal percentage valve applies.

$$\dot{n}_{recflo} = \text{Position}_{recvalv} \sqrt{\frac{298}{gT_u}} C_g P_u \sin\left\{ \frac{3417}{C_1} \sqrt{\left(\frac{P_u - P_d}{P_u} \right)} \right\}_{degrees} \quad -(4.10)$$

4.1.4 Block Valve Flowrate

The flow through each of the block valves is a function of the flow through the compressor and the position of the valve. Forward flow is assumed because as the compressor slows down, the gas feeding the compressor will increase in pressure and the discharge gas exiting the compressor will decrease in pressure. In addition the discharge check valve will prevent any reverse flow. Reverse flow is also prevented by the compressor valves which only allow unidirectional flow forwards through the compressor. Thus, the flow through the valve is assumed to be linear with compressor flowrate as shown in equation 4.11.

$$\dot{n}_{\text{floESDV}} = \dot{n}_{\text{compflo}} \text{Position}_{\text{ESDV}} \qquad -(4.11)$$

4.1.5 Compressor Flowrate

While the compressor is running, and the discharge pressure is greater than the suction pressure, the flowrate through the compressor is a linear function of compressor speed. The compressor speed is predicted from the compressor rundown section of the program as described in section 4.4.

$$\dot{n}_{\text{compflo}} = \frac{RPM}{\text{MaxRPM}} \text{FloMax} \qquad -(4.12)$$

When the compressor is shut down and the discharge pressure is equal to the suction pressure the gas flowrate through the compressor is assumed to be sufficient to equalize suction and discharge piping. This assumption is necessary because the equations governing the compressor valve flow characteristics are considered proprietary knowledge by the valve manufacturers.

4.1.6 Pressure Prediction

The pressures were predicted using the compressibility factors from the Lee Kesler equation of state. The new pressure for time t+1 is predicted from the property values at time t and t+1. The values for t+1 are first guessed and recalculated in the internal loop (m) until convergence. Convergence criteria is governed by the following equation:

$$\frac{\text{Pressure}(m) - \text{Pressure}(m-1)}{\text{Pressure}(m)} \leq \text{tolerance}$$

The tolerance was set at 0.01. When the pressure in the flare header, discharge piping, and suction piping balance are met to within the convergence criteria the program increments to the next time step and the m loop counter was reset (m=1). The loop counter was limited to ten iterations

however convergence was usually achieved in three iterations. If convergence could not be achieved, the program time step was reduced by half.

Equation 4.13 represents the equation for the conservation of volume:

$$P_{t+1} = \frac{n_{t+1} P_t T_{t+1} Z_{t+1}}{Z_t T_t n_t} \qquad -(4.13)$$

The value of the pressure is calculated for succeeding iterations of time. In each iteration the mole balance is performed on the new flowrates calculated from the preceding values of pressure. The discharge pressure decreases rapidly as the depressuring process proceeds. When the discharge pressure equals the interstage pressure the moles of interstage gas are added to the remaining discharge moles and the depressuring proceeds.

4.2 FLARE SYSTEM

The flare system flowrates are calculated according to equations 4.9 or 4.10 depending on the type of valve. The flare system temperature and pressure are calculated as shown in the following sections.

4.2.1 Flare System Pressure

The flare system pressure is calculated according to Darcy's Law[4]. First Reynold's number is calculated and used to estimate the friction factor.

$$Re = \frac{\rho \cdot D \cdot vel_{flar}}{\mu} \qquad -(4.14)$$

The friction factor is estimated according to equation 4.15 for the first iteration. For each succeeding iteration the value of the preceding iteration is used in equation 4.16.

$$f_{guess} = \frac{64}{Re} \qquad -(4.15)$$

The new value of the friction factor is calculated by the Colebrook equation assuming a roughness for new steel pipe.

$$f_{new} = 1.0/\left(-2\log\left\{\frac{0.061}{3.7D} + \frac{2.51}{Re\sqrt{f_{guess}}}\right\}\right) \qquad -(4.16)$$

The lost head can be calculated from equation 4.17 and used in equation 4.18 to calculate the pressure drop.

$$h = f\frac{L}{D}\frac{Vel^2}{2g_c} \qquad -(4.17)$$

$$\Delta P = \rho h g \qquad -(4.18)$$

Flare systems often have more than one diameter of pipe, so that it becomes necessary to calculate the pressure drop in two stages. The first stage is from atmospheric pressure to the diameter change. The second stage is from the diameter change to the depressuring source.

4.2.2 Flare System Temperature

The temperature in the flare system is calculated by performing an isenthalpic calculation across the throttling valve. This is an iterative procedure using the ratio of enthalpies to predict the new temperature as shown in equation 4.19. The initial temperature is set at 90% of the upstream. Convergence was normally achieved in three iterations.

$$\left(T_d\right)_{t+1} = \frac{H_u}{H_d}\left(T_d\right)_t \qquad -(4.19)$$

4.2.3 Flare System Viscosity

Once the downstream temperature is predicted the viscosity is calculated[5] as per equations 4.20 to 4.22. The viscosity correlation is not corrected for pressure but it is considered valid over the range of pressures exhibited in the flare system.

IF $T_r < 1.5$ THEN

$$\mu_{mix} = \frac{3.4 T_r^{8/9}}{\epsilon_{mix}} \qquad -(4.20)$$

IF $T_r > 1.5$ THEN

$$\mu_{mix} = \frac{16.68}{\epsilon_{mix}} (0.1338 T_r - 0.0932)^{5/9} \qquad -(4.21)$$

where:

$$\epsilon_{mix} = \frac{T_{cm}^{1/6}}{P_{cm}^{2/3}} MW_{mix} \qquad -(4.22)$$

4.3 DEPRESSURING TIME

The depressuring time is defined as the time for the system to depressure to an arbitrary final pressure. It may not be possible to achieve the final pressure because of a high flare header pressure. The high flare header pressure is caused by gases in the flare header from other sources.

However for this study the final pressure for this study was selected as 345 kPa (abs) for the Reinjection compressor and 155 kPa (abs) for the Cardium compressor. The final pressure selected depends on the suction piping maximum operating pressure. High pressure systems require a smaller flare valve because of the high initial flare flowrate. Therefore, the high pressure system depressurizes at a slower rate than the low pressure system.

Depressuring time is calculated from the pressure transient analysis outlined in section 4.1. The steps in the depressuring sequence (mole balance, flare flowrate, and pressure calculation) are repeated until the system pressure equals the final pressure or the flare header back pressure.

4.4 RUNDOWN TIME CALCULATIONS

The rundown calculations were developed from the mechanics of the compressor. The compressor acts as a slider crank mechanism as shown in Figure 4.1. The development of the equations used in the compressor rundown calculations are shown in sections 4.4.1 to 4.4.4.

4.4.1 Piston Travel

For any angle of the crank the travel of the piston is determined from equation 4.23.[5]

$$X_B = (R_2 + R_3) - \left\{ R_2 \cos\theta_2 + R_3 \left\{ \cos\left(\sin^{-1}\left(\frac{R_2}{R_3} \sin\theta_2 \right) \right) \right\} \right\} \qquad -(4.23)$$

4.4.2 Displacement Volume and Cylinder Pressure

Once the travel is determined at each crank angle the displacement volume is calculated. The total displacement volume including the fixed cylinder clearance is calculated for each cylinder by equations 4.24 and 4.25.

The head end volume is calculated as a function of the piston travel and the dimensions of the piston and the fixed clearance at the head end of the piston travel.

$$V_{HEcyl} = 2\left(\frac{\pi}{4}\right) D_{pist}^2 X_B + \text{ClearanceVol}_{HE} \qquad -(4.24)$$

The crank end volume is calculated as a function of the piston travel and the dimensions of the piston and the fixed clearance at the crank end of the piston travel.

$$V_{CEcyl} = 2\left(\frac{\pi}{4}\right)\left(D_{pist}^2 - D_{rod}^2\right) X_B + \text{ClearanceVol}_{CE} \qquad -(4.25)$$

SLIDER CRANK DIAGRAM FOR 2 STAGE COMPRESSOR

FIGURE 4.1

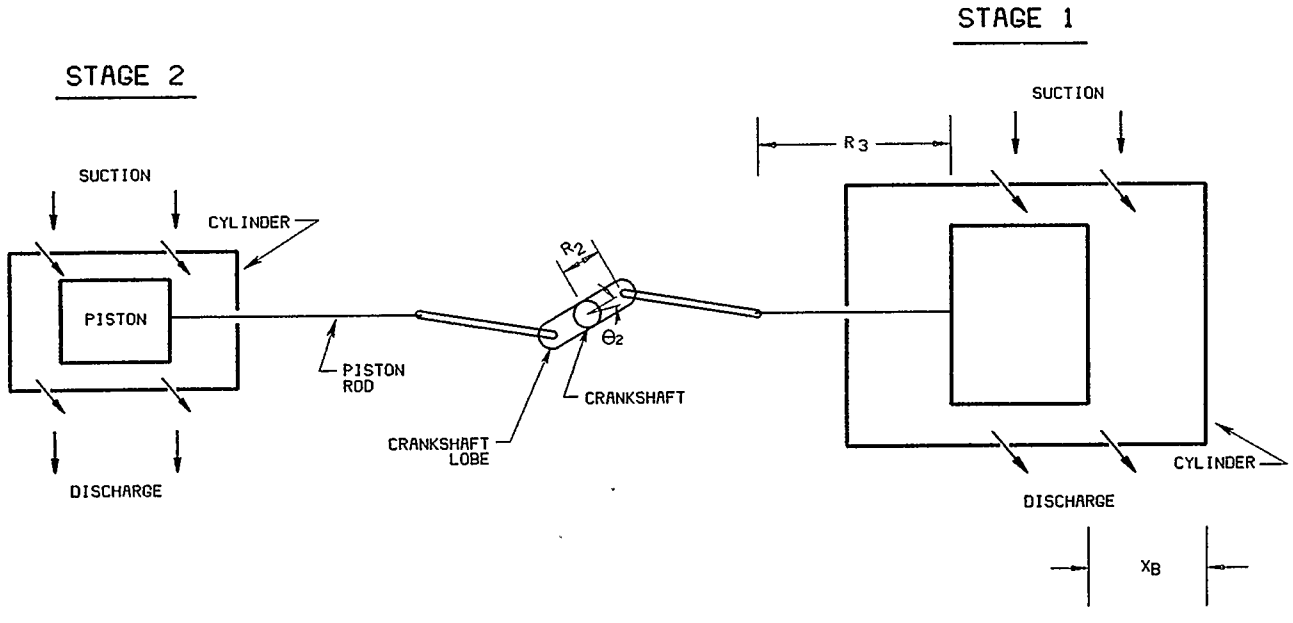

The constant for each end of both cylinders is calculated by evaluating equation 4.26 at the initial value of temperature and pressure. Assuming isentropic compression, the pressure for each crank angle is then determined according to equation 4.26.

$$P_{cyl} V_{cyl}^{k} = \text{constant} \qquad -(4.26)$$

The cylinder pressure is limited by the suction or discharge pressure depending on which end of the stroke the piston is at. As the discharge pressure decreases the cylinder pressure decreases. This decreasing cylinder pressure reduces the braking action of the piston and increases the compressor rundown time.

4.4.3 Torque

The torque is calculated for each crank angle using the pressure calculated from equation 4.26 and from equations 4.27 and 4.28 which were developed from the mechanics of the slider crank mechanism.

Head end torque is calculated from the geometry of Figure 4.1 and given by equation 4.27:

$$\tau = \left(\frac{\pi}{4}\right) D_{pist}^2 P_{cyl} \sin\theta_2 R_2 \qquad -(4.27)$$

Equation 4.28, the crank end torque is calculated from the compressor geometry shown in Figure 4.1.

$$\tau = \left(\frac{\pi}{4}\right)\left(D_{pist}^2 - D_{rod}^2\right) P_{cyl} \sin\theta_2 R_2 \qquad -(4.28)$$

The total torque is a summation of the torque from both sides of each cylinder.

4.4.4 Compressor Speed and Run Down Time

After the power to the driver is terminated the total torque acts as a brake to stop the compressor. The time to stop the compressor depends on the system inertia as shown in equation 4.29.

$$\omega_{new} = \left\{\left(0.5 \cdot I \cdot \omega_{old}^2\right) - \frac{\tau_{tot}}{0.5 \cdot I}\right\}^{0.5} \qquad -(4.29)$$

The procedure is based on an iteration of crank angle. That is, for every 15 degrees of rotation new values of pressure and torque are generated and a new rpm is predicted. In this way the total time for rundown can be calculated as a

sum of the time required for the compressor to rotate 15 degrees for each time t. The compressor rundown time is about 0.5 seconds for small systems with low inertia to 10 seconds for larger systems with high inertia.

4.5 RECYCLE VALVE FAIL POSITION

The fail position of the recycle valve has a dramatic effect on suction pressures during the depressuring sequence. If the valve fails open, the gas volume is transferred from the discharge to suction as described by equation 4.11. This can cause the suction pressure piping to be overpressured.

The suction piping PSV must be sized to accommodate the maximum flare flowrates necessary to maintain the suction pressure below the suction piping maximum operating pressure. The recycle flowrate prediction is difficult because the upstream (discharge) pressure is decreasing rapidly and the downstream pressure is increasing rapidly. If the system is small, the valve may not be fully open before the upstream and downstream pressures equalize. The combination of assuming a full open recycle valve and a high initial system pressure will result in the selection of a large suction PSV. Consequently a larger investment will be required for both the PSV and the flare header piping.

The effect of failing the recycle valve open was predicted by incorporating a fail open recycle position into the pressure transient analysis.

4.6 SUCTION FLARE VALVE

The installation of a flare valve on the suction piping is believed to decrease the depressuring time. This concept was investigated by applying the applicable flare flowrate equation 4.9 or 4.10, and calculating the suction flare flowrate. The suction flare flowrate affects the mole balance in equation 4.1 and the suction pressure calculation. At later times in the depressuring sequence, it will affect the mixture volumes when the pressure from the discharge is equal to the suction pressure.

4.7 EMERGENCY SHUT DOWN BLOCK VALVES

The Emergency Shut Down Block Valves (ESDVs), shown in Figure 4.2, are designed to isolate the compressor station in the event of an emergency. The ESDVs are generally ball valves equipped with pneumatic actuators. Power gas or instrument air enters the cylinder via the solonoid valve and compresses the actuator spring and opens or closes the valve. The ESDV is a "fail safe" system because the spring will return the valve to the "safe" position upon power gas

loss or solonoid failure. The rate of closure depends on the volume of the actuator and the port size in the solonoid vent line. The location of the actuator and solonoid are shown in Figure 4.2

EMERGENGY SHUTDOWN BLOCK VALVE

FIGURE 4.2

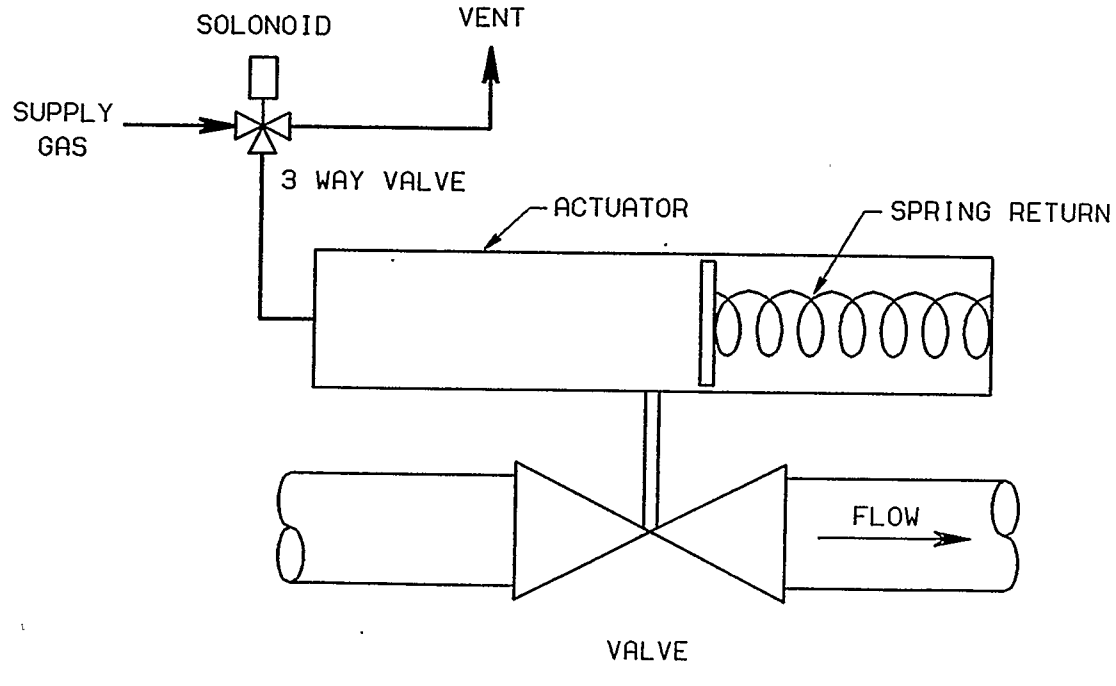

The time for the actuator to close can be predicted using the Fisher Valve sizing equation 4.9. For sonic flow this equation reduces to equation 4.30.

$$Q = CgP_u\left\{\frac{298}{gT_u}\right\}^{0.5} \qquad -(4.30)$$

If the flowrate is constant, the mole balance from time 1 to time 2 can be rearranged to equation 4.31[7].

$$Q = \frac{RT}{P_{sc}}\frac{(n_2 - n_1)}{t} \qquad -(4.31)$$

Assuming an ideal gas and an isothermal process, with a constant discharge temperature, the mole balance can be related to volume in equations 4.32 and 4.33.

$$n_2 = \frac{P_2 V}{RT} \qquad -(4.32)$$

$$n_1 = \frac{P_1 V}{RT} \qquad -(4.33)$$

Then combining equations 4.31,4.32 and 4.33 results in equation 4.34.

$$t = \frac{V(P_2 - P_1)}{QP_{sc}} \qquad -(4.34)$$

For an infinitesimally small time period differentiating equation 4.34 results in the following equation.

$$\partial t = \frac{V}{QP_{sc}} \partial P \qquad -(4.35)$$

Substituting equation 4.30 into equation 4.35 results in equation 4.36.

$$\int_0^t \partial t = \int_{Pu_2}^{Pu_1} \frac{V}{CgP_{sc}\sqrt{298/(gT_u)}P_u} \partial P \qquad -(4.36)$$

Integrating equation 4.36 results in equation 4.37 which allows the depressuring time from the upstream pressure at time 1 (Pu_1) to the upstream pressure at time 2 (Pu_2) in hours to be calculated.

$$t = \frac{V}{CgP_{sc}} \sqrt{\frac{gT_u}{298}} \ln\left(\frac{Pu_1}{Pu_2}\right) \qquad -(4.37)$$

The valve position is normally expressed as a linear function of time as shown in equation 4.38.

$$Position = t / t_{travel} \qquad -(4.38)$$

The subsonic portion does not need to be considered, because the valve will be almost closed before the subsonic flow becomes predominant.

CHAPTER 5

THERMODYNAMICS PROPERTY PACKAGE

The thermodynamic property package was developed to enhance the models capability to predict pressures due to the large variations in compressibility (Z) and heat capacity ratio (K).

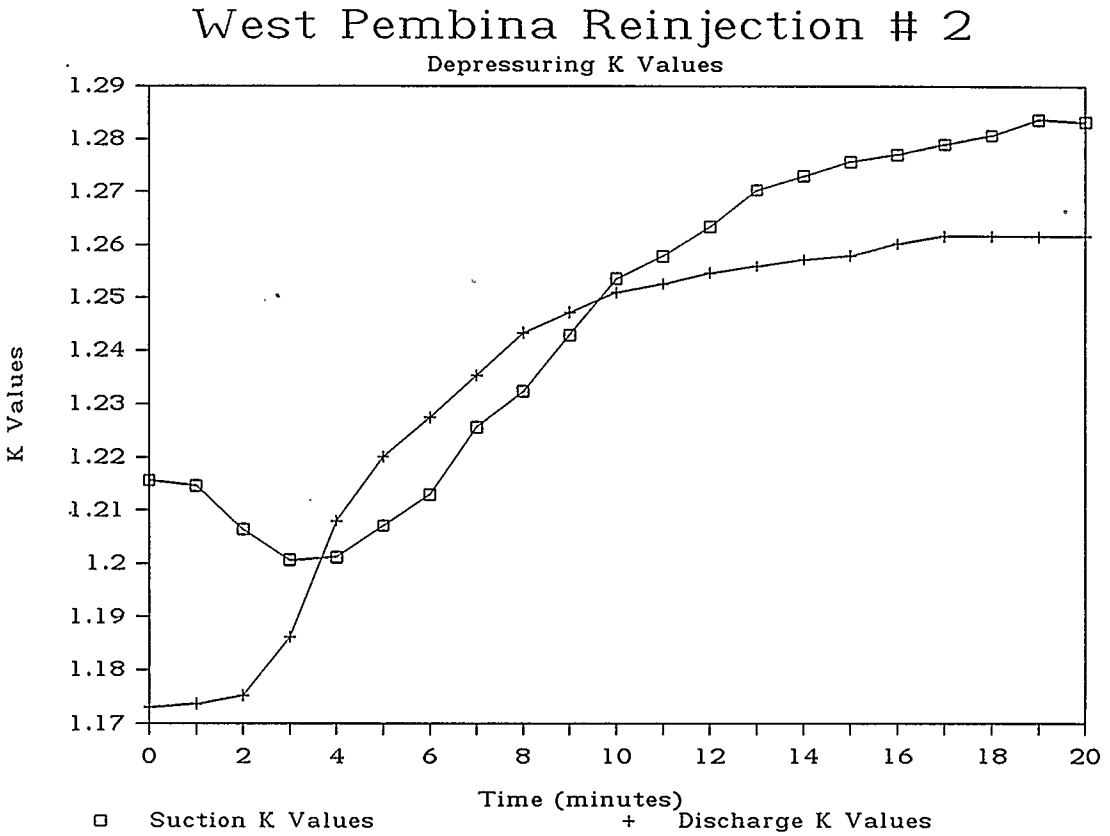

FIGURE 5.1

In Figures 5.1 and 5.2 the suction and discharge values of K and compressibility-temperature product (ZT) are shown as a

function of time. The values were calculated using Hysim at the temperature and pressure measured. The maximum error when assuming an average K value of 1.23 is 5.1%. The maximum error when assuming an average ZT value of 290 Kelvin is 31.8%. The model was originally developed using average properties, however the pressure transient match was not satisfactory. The thermodynamic property package was then developed to achieve a better pressure prediction.

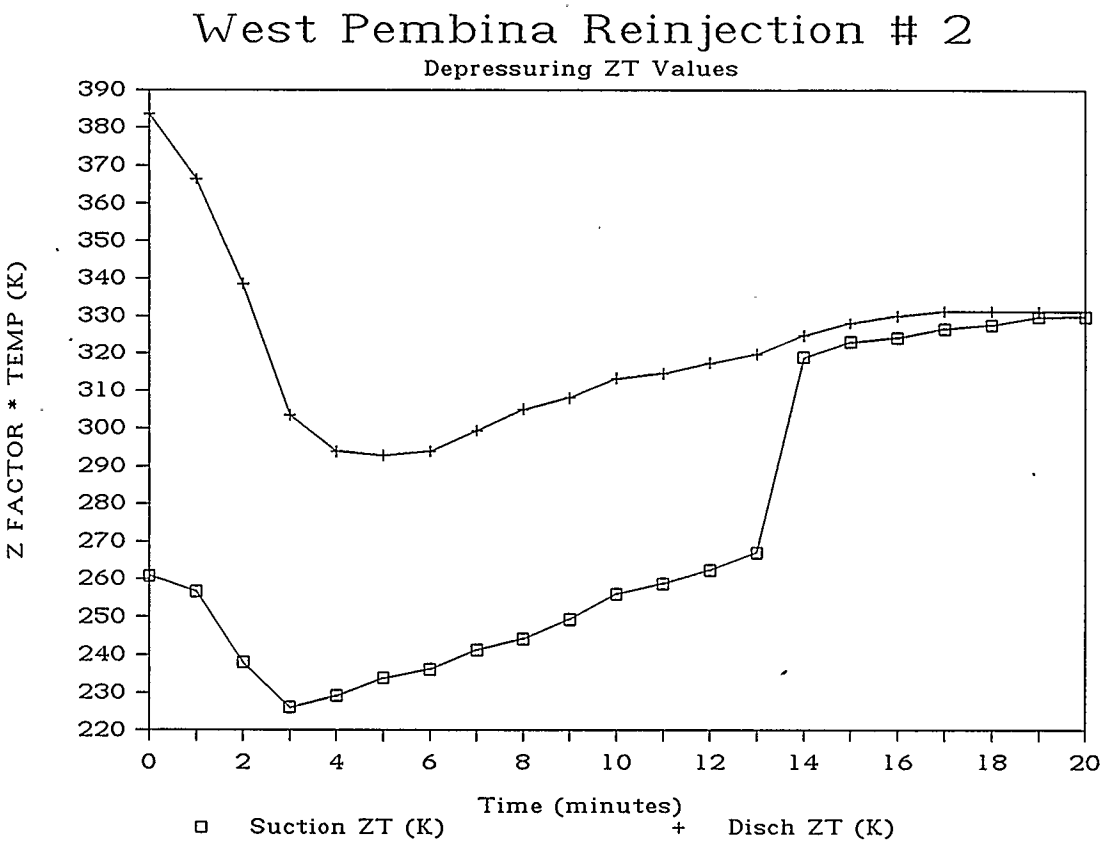

FIGURE 5.2

The thermodynamic calculations are based on a three parameter corresponding states correlation developed by Lee and Kesler[8]. For each successive iteration of the time (t) loop the properties (Z,K,viscosity and enthalpy) are evaluated. In addition these properties are also evaluated for each of the successive iterations of the internal (m) loop.

It should be noted that the property package was only developed for the gas phase. However, this is quite adequate because compressors can only operate properly in the gas phase.

5.1 COMPRESSIBILITY FACTOR

The compressibility factor is calculated using equation 5.1[8] and using hexane as a reference fluid.

$$Z = Z^{(0)} + \frac{\omega}{\omega^{(r)}}\left(Z^{(r)} - Z^{(0)}\right) \qquad -(5.1)$$

where:

$\omega^{(r)} = 0.3978$

Compressibility was first calculated for the simple fluid (0) and then for the reference fluid (r). The first step was to iteratively calculate the value for $Vr^{(0)}$ for a simple fluid using equation 5.2. The simple fluid value of $Vr^{(0)}$ was calculated by using the simple fluid values from Table 5.1 to calculate $B^{(0)}$, $C^{(0)}$, $D^{(0)}$ from equations 5.4 to 5.6.

$$V_r = \left\{\frac{T_r}{P_r}\right\}\left\{1 + \frac{B}{V_r} + \frac{C}{V_r} + \frac{D}{V_r} + \frac{c_4}{T_r^3 V_r^2}\left\{\beta + \frac{\gamma}{V_r^2}\right\}\exp\left(-\frac{\gamma}{V_r^2}\right)\right\} \qquad -(5.2)$$

Then $Z^{(0)}$ can be calculated from equation 5.3 using the simple fluid value of $Vr^{(0)}$

$$Z = \left\{ \frac{P_r V_r}{T_r} \right\} \qquad -(5.3)$$

This procedure was repeated for the reference fluid.

$$B = b_1 - \frac{b_2}{T_r} - \frac{b_3}{T_r^2} - \frac{b_4}{T_r^3} \qquad -(5.4)$$

$$C = c_1 - \frac{c_2}{T_r} + \frac{c_3}{T_r^3} \qquad -(5.5)$$

$$D = d_1 + \frac{d_2}{T_r} \qquad -(5.6)$$

The values used for b,c and d are in Table 5.1.

Table 5.1

Constants for Lee Kesler Equations[8]

Constant	Simple Fluid	Reference Fluid
b_1	0.1181193	0.2026579
b_2	0.2657280	0.3315110
b_3	0.1547900	0.0276550
b_4	0.0303230	0.2034880
c_1	0.0236744	0.0313385
c_2	0.0186984	0.0503618
c_3	0.0000000	0.0169010
c_4	0.0427240	0.0415770
$d_1 \times 10^4$	0.1554880	0.4873600
$d_2 \times 10^4$	0.6236890	0.0740336
β	0.6539200	1.2260000
γ	0.0601670	0.0375400

5.2 ENTHALPY DEPARTURE

The enthalpy departure was calculated using equations 5.7 to 5.9[8].

$$H - \frac{H^\circ}{RT_c} = T_r\{Z - 1 - \frac{b_2 + 2b_3/T_r + 3b_4/T_r^2}{T_r V_r} -$$

$$\frac{c_2 - 3c_3/T_r^2}{2T_r V_r^2} + \frac{d_2}{5T_r V_r^5} + 3E\} \qquad -(5.7)$$

where:

$$E = \frac{c_4}{2T_r^3\gamma}\left\{\beta + 1 - \left(\beta + 1 + \frac{\gamma}{V_r^2}\right)\exp\left(-\frac{\gamma}{V_r^2}\right)\right\} \qquad -(5.8)$$

The enthalpy departure was calculated by using equation 5.7 for a simple fluid, a reference fluid, and then using equation 5.9.

$$\left\{\frac{H - H^\circ}{RT_c}\right\} = \left\{\frac{H - H^\circ}{RT_c}\right\}^{(0)} + \left(\frac{\omega}{\omega^{(r)}}\right)\left\{\frac{H - H^\circ}{RT_c}\right\}^{(r)} - \left\{\frac{H - H^\circ}{RT_c}\right\}^{(0)} \qquad -(5.9)$$

The required ideal enthalpy was calculated from equation 5.10[5].

$$H^\circ = \sum x_i\left(Cp_A T + Cp_B\frac{T^2}{2} + Cp_C\frac{T^3}{3} + Cp_D\frac{T^4}{4}\right)_i \qquad -(5.10)$$

5.3 ISOCHORIC HEAT CAPACITY DEPARTURE

The isochoric heat capacity was calculated from equation 5.11[8].

$$\frac{Cv - Cv^{\circ}}{R} = \frac{2\left(b_3 + 3b_4/T_r\right)}{T_r^2 V_r} - 3\frac{c_3}{T_r^3 V_r^2} - 6E \qquad -(5.11)$$

5.4 ISOBARIC HEAT CAPACITY

The isobaric heat capacity departure was calculated from equations 5.12 to 5.14[8].

$$\frac{Cp - Cp^{\circ}}{R} = \frac{Cv - Cv^{\circ}}{R} - 1 - T_r\left(\frac{\partial P_r}{\partial T_r}\right)_{V_r}^2 \Big/ \left(\frac{\partial P_r}{\partial V_r}\right)_{T_r} \qquad -(5.12)$$

The required values of the partial differentials in equation 5.12 were evaluated as follows.

The partial differential with respect to temperature is calculated from equation 5.13.

$$\left(\frac{\partial P_r}{\partial T_r}\right)_{V_r} = \frac{1}{V_r}\left\{\left(1 + \frac{b_1 + b_3/T_r^2 + 2b_4/T_r^3}{V_r} + \frac{c_1 - 2c_3/T_r^3}{2V_r^2} + \right.\right.$$
$$\left.\left.\frac{d_1}{5V_r^5} - \frac{2c_4}{T_r^3 V_r^2}\right)\left\{\left(\beta + \frac{\gamma}{V_r^2}\right)\exp\left(-\frac{\gamma}{V_r^2}\right)\right\}\right\} \qquad -(5.13)$$

The partial differential with respect to volume is calculated as shown in equation 5.14.

$$\left(\frac{\partial P_r}{\partial V_r}\right)_{T_r} = -\frac{T_r}{V_r^2}\left\{\left(1+\frac{2B}{B_r}+\frac{3C}{V_r^2}+\frac{6D}{V_r^5}+\frac{c_4}{T_r^3 V_r^2}\right.\right.$$
$$\left.\left.\left\{3\beta+\left\{5-2\left(\beta+\frac{\gamma}{V_r^2}\right)\right\}\right\}\right)\frac{\gamma}{V_r^2}\right\}\exp\left(-\frac{\gamma}{V_r^2}\right) \qquad -(5.14)$$

The ideal isobaric heat capacity was evaluated from equation 5.15[5].

$$Cp^{\circ} = \sum x_i\left(Cp_A + Cp_B T + Cp_C T^2 + Cp_D T^3\right)_i \qquad -(5.15)$$

5.5 HEAT CAPACITY RATIO

The heat capacity ratio was calculated using equation 5.16.

$$K = \frac{Cp}{Cp - R} \qquad -(5.16)$$

5.6 MIXING RULES

When using the Lee Kesler correlations it is important to use the Lee Kesler mixing rules[8], the mixing rules are used to define the critical properties of the mixture as given by the following equations.

$$V_{ci} = \frac{Z_{ci} R T_{ci}}{P_{ci}} \qquad -(5.17)$$

$$Z_{ci} = 0.2905 - 0.085\omega_i \qquad -(5.18)$$

$$V_c = \frac{1}{8}\sum_k \sum_j x_j x_k \left(V_{cj}^{1/3} + V_{ck}^{1/3}\right)^3 \qquad -(5.19)$$

$$T_c = \frac{1}{8V_c}\sum_k \sum_j x_j x_k \left(V_{cj}^{1/3} + V_{ck}^{1/3}\right)^3 \sqrt{T_{cj} T_{ck}} \qquad -(5.20)$$

$$\omega = \sum_j x_j \omega_j \qquad -(5.21)$$

$$P_c = \frac{Z_c R T_c}{V_c} = (0.2905 - 0.085\omega)\left\{\frac{R T_c}{V_c}\right\} \qquad -(5.22)$$

CHAPTER 6

RESULTS AND DISCUSSION

The results of the study are presented in three sections. In the first section the pressure transient analysis prediction is compared to the recorded data for both the Reinjection Compressor #2 and the Cardium compressor. In the second section the predicted rundown time and valve travel time are compared to measured results. In the third section the thermodynamic property predictions are compared to literature values.

The Data Tables associated with Figures 6.1 through 6.12 are attached in Appendix A.

6.1 PRESSURE TRANSIENT ANALYSIS

The predicted pressure transient analysis for both compressors were verified by comparing the predicted pressure to the pressure measured for the industrial compressors. After demonstrating the model's capability to predict pressure transients, the model was used to predict the effect of hypothetical changes to the design of Reinjection Compressor #2.

6.1.1 Reinjection Compressor Measured Data

The data recorded from the shut down and depressuring of the Reinjection Compressor #2 are shown in Figure 6.1. The data was recorded by the Bailey Network 90 control system at the West Pembina plant in June 1987. The data as recorded for Reinjection Compressor #2 is attached as Appendix B.

Figure 6.1 is composed of three curves. The uppermost curve is the pressure of the discharge piping. The discharge pressure initially exhibits a rapid rate of depressuring. The interstage and suction pressure remain essentially constant until the discharge pressure is low enough to allow flow from the interstage piping to the discharge piping and eventually from suction piping to interstage piping. Because of the check valve action of the compressor valves gas is only allowed to flow forward through the compressor. Therefore the discharge piping can never flow back into the interstage piping and cause the compressor to run backwards.

The rate of pressure decline is dependent on flare flowrate and the piping volume being depressured. At the time of equalization of the interstage and discharge pressures the rate of decline is slowed because of the added volume that

is now being flared from the discharge flare valve. The flare flowrate remains constant but the volume base has increased.

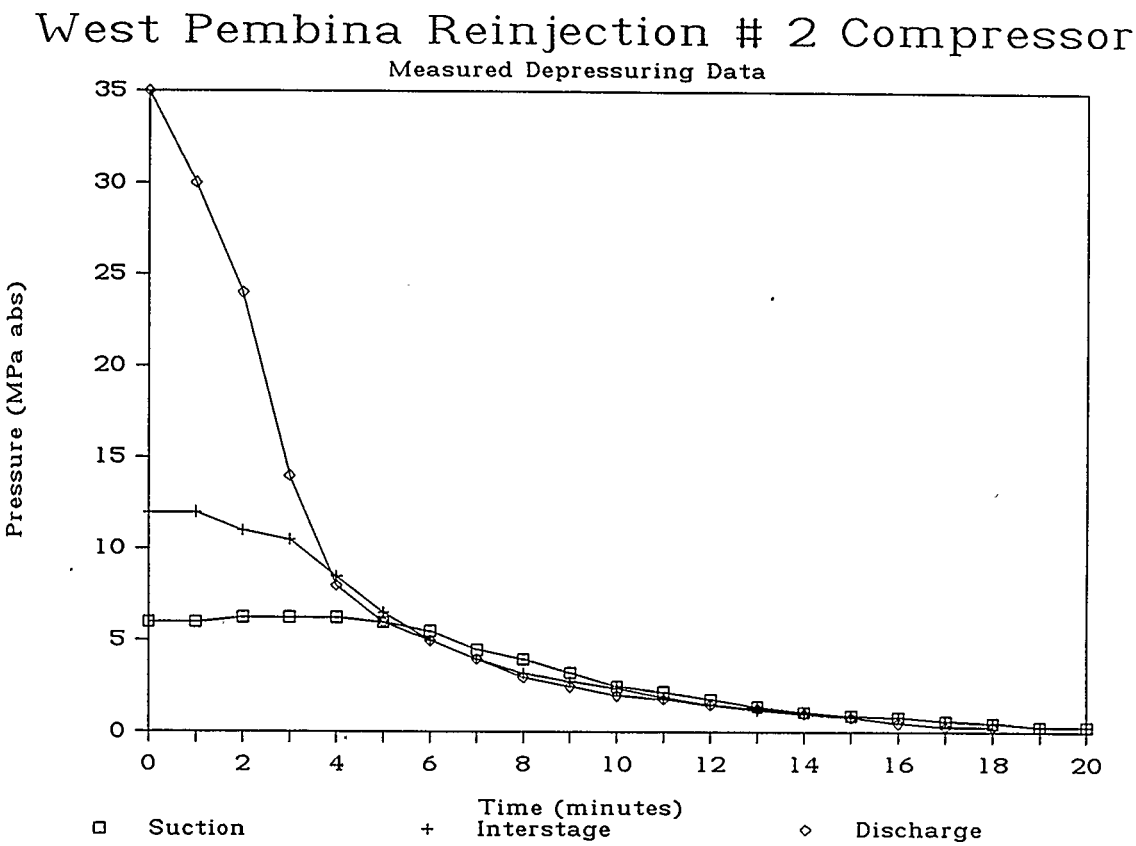

FIGURE 6.1

The initial rate of decline is limited by the maximum flowrate the flare system can handle. The design flare flowrate is restricted because Reinjection Compressor #2 shares the flare system with the entire plant. During an

emergency shut down, the pressure within the entire flare system must not exceed 450 kPa abs. Therefore Reinjection Compressor #2 is only allotted a portion of the flare system capacity. The flare header pressure could not be measured because there are no pressure tap connections in the flare piping, thus the predicted flare header pressure drop could not be verified for Reinjection Compressor #2. In section 6.1.10 the Cardium Compressor flare header pressure drop calculation was verified.

6.1.2 Reinjection Compressor Pressure Match

In Figures 6.2a, 6.2b, and 6.2c the predicted pressures are matched against the recorded data.

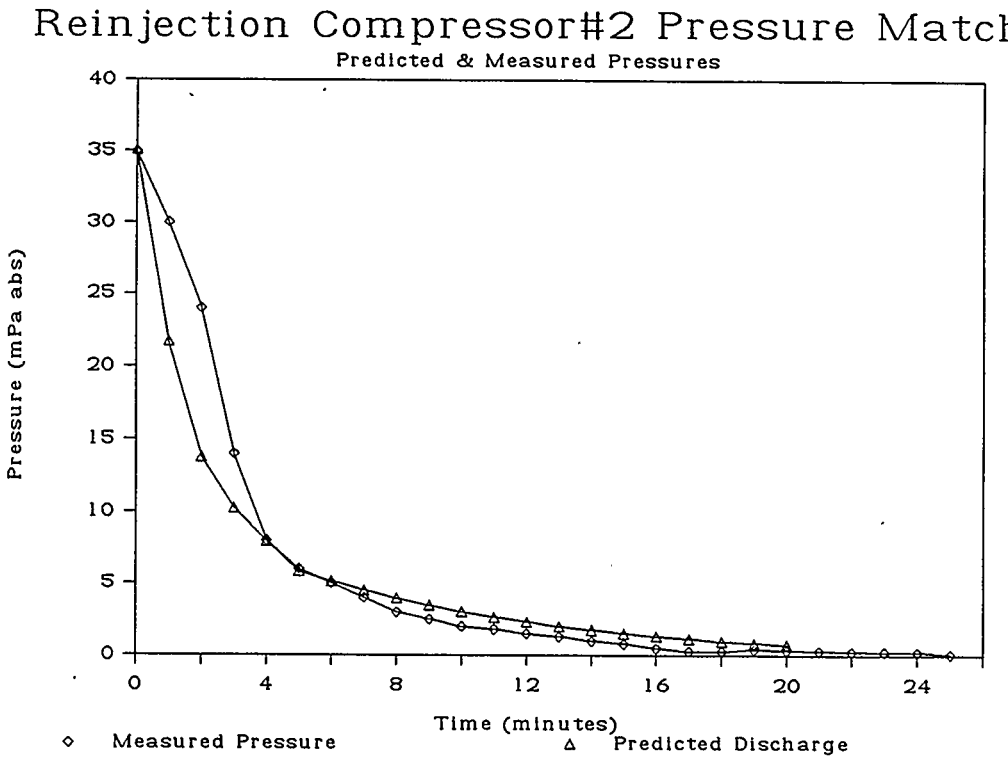

FIGURE 6.2a

In Figure 6.2a the measured discharge pressure begins to decline at a later time than the predicted discharge pressure. This is the result of the discharge flare valve opening slower than predicted. The rate of pressure decline begins to decrease as the discharge pressure and interstage pressure equalize.

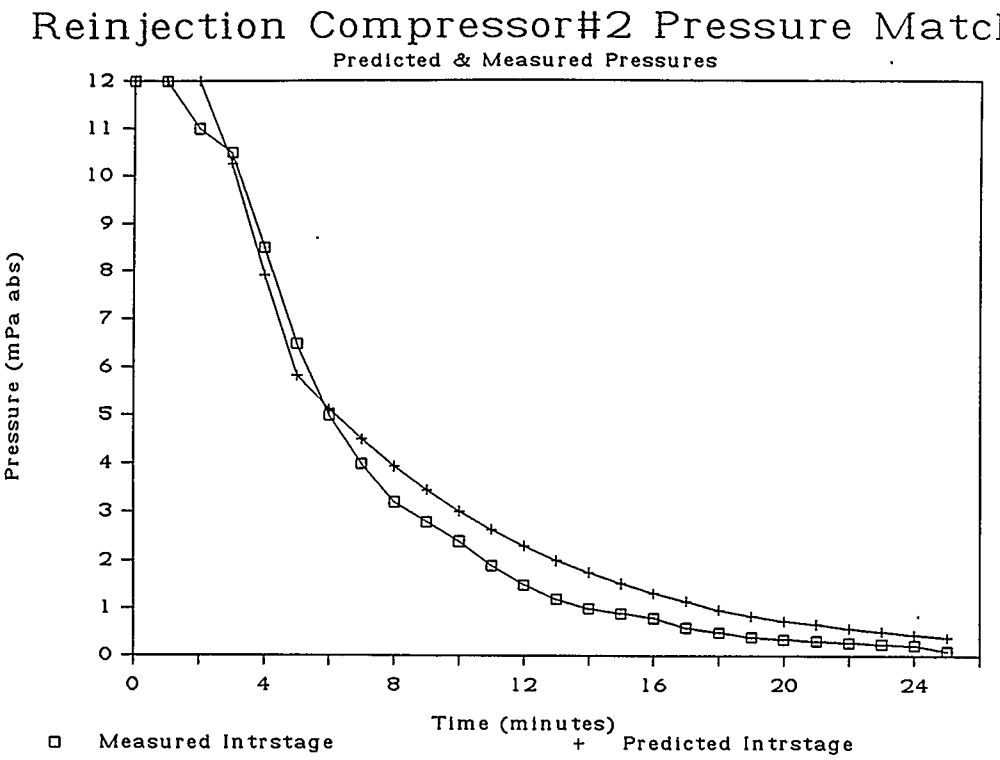

FIGURE 6.2b

Figure 6.2b shows the measured interstage pressure compared to the predicted interstage pressure. The predicted interstage pressure matches the measured pressure up to the second equalization. After the second equalization, the predicted interstage and suction pressures are higher than the measured pressures. This error is discussed following Figure 6.2c.

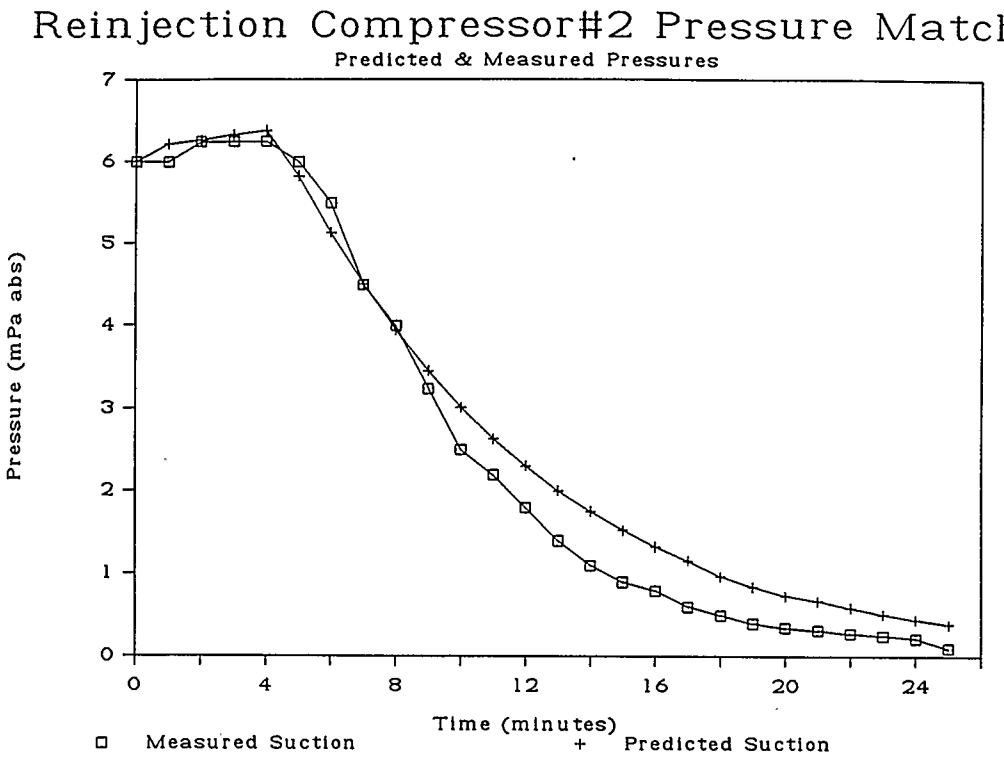

FIGURE 6.2c

Figure 6.2c shows the measured suction pressure rising less than the predicted suction pressure in the first portion of the graph. This is caused by the predicted flow of gas through the suction ESDV being higher than the actual flow of gas. This error is propagated into the later time pressure prediction because there is now an additional volume of gas in the system which has to be flared from the discharge flare valve.

The calculated depressuring time to 345 kPa abs was 25 minutes, and the actual time was 20 minutes.

The predicted maximum flare flowrate was 309.87 $10^3m^3_{sc}/day$ at a maximum flare header pressure of 126.2 kPa abs. The maximum flare header pressure was calculated assuming no gas from other sources within the flare system were going to flare, during the test.

6.1.3 Cardium Compressor Measured Data

In Figure 6.3 the measured depressuring data for the Cardium Compressor is presented. The data was recorded manually from pressure gauges during the depressuring sequence.

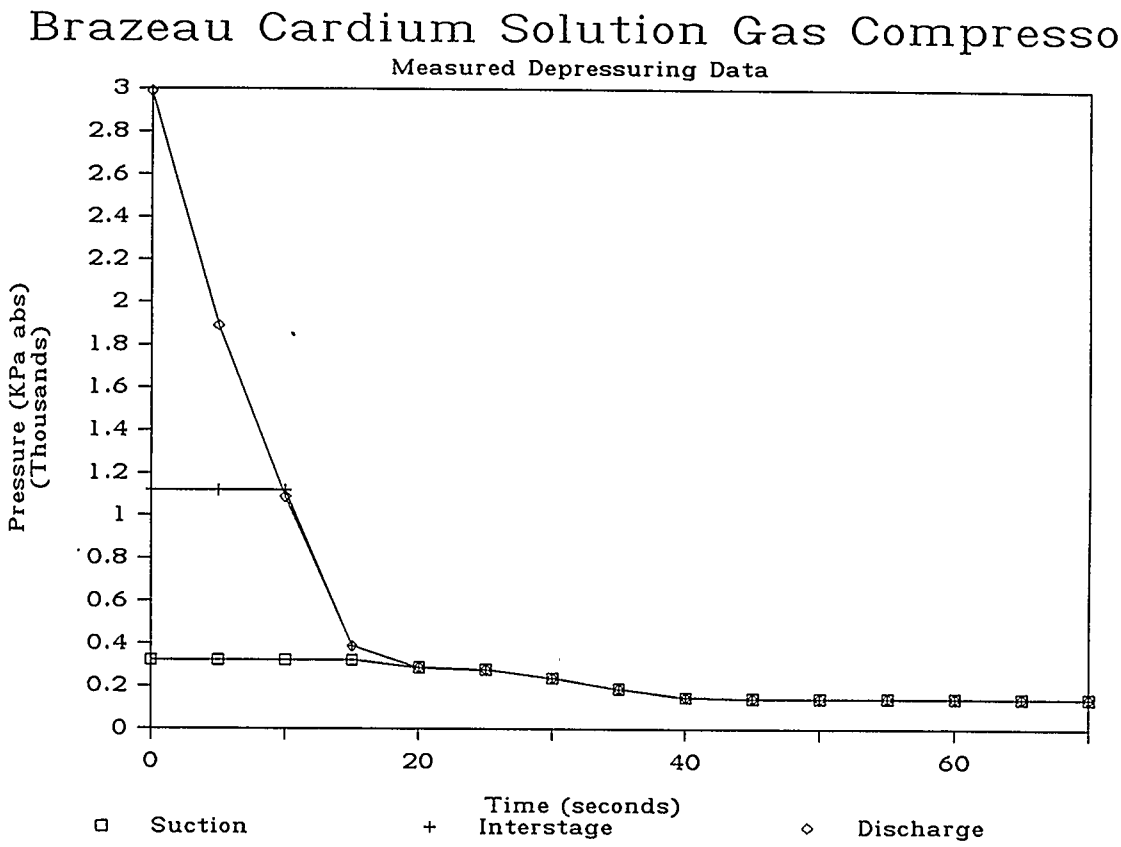

FIGURE 6.3

Figure 6.3 shows the same three rate depressuring curves as was exhibited by Reinjection Compressor #2. The first equalization occurs when the discharge pressure equalizes to

the interstage pressure. The second equalization occurs when the discharge pressure equalizes to the suction pressure.

The Cardium system starts with a lower initial pressure of 3,000 kPa abs and has a smaller volume of piping relative to Reinjection Compressor #2. Because the total volume of the system is smaller and the initial flare flowrate is relatively higher, there is a smaller change in the rate of depressuring for each stage during pressure equalization. The Cardium compressor is allowed a relatively higher initial flare flowrate because it is not integrated with other processes during a total plant emergency depressuriza-tion.

6.1.4 Cardium Compressor Pressure Match

Figures 6.4a, 6.4b and 6.4c demonstrates the model's capability to predict the pressures for a smaller system with a rapid pressure decline.

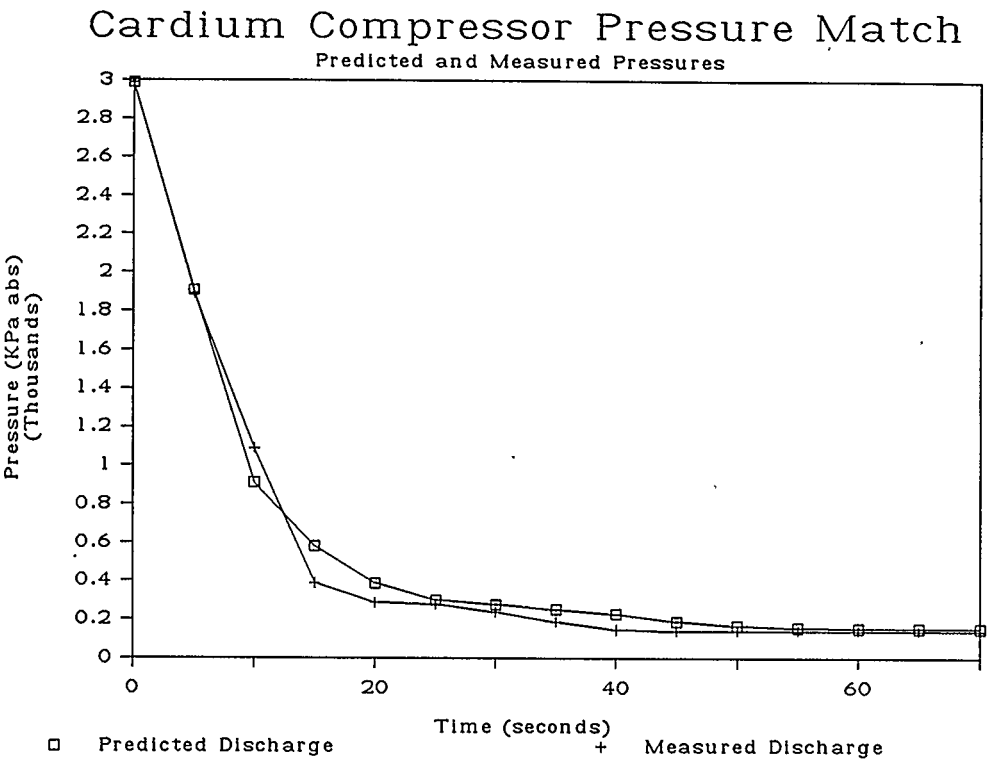

FIGURE 6.4a

Figure 6.4a shows the measured discharge pressure compared to the predicted discharge pressure. The initial pressure match is the result of a better prediction of discharge flare valve opening time.

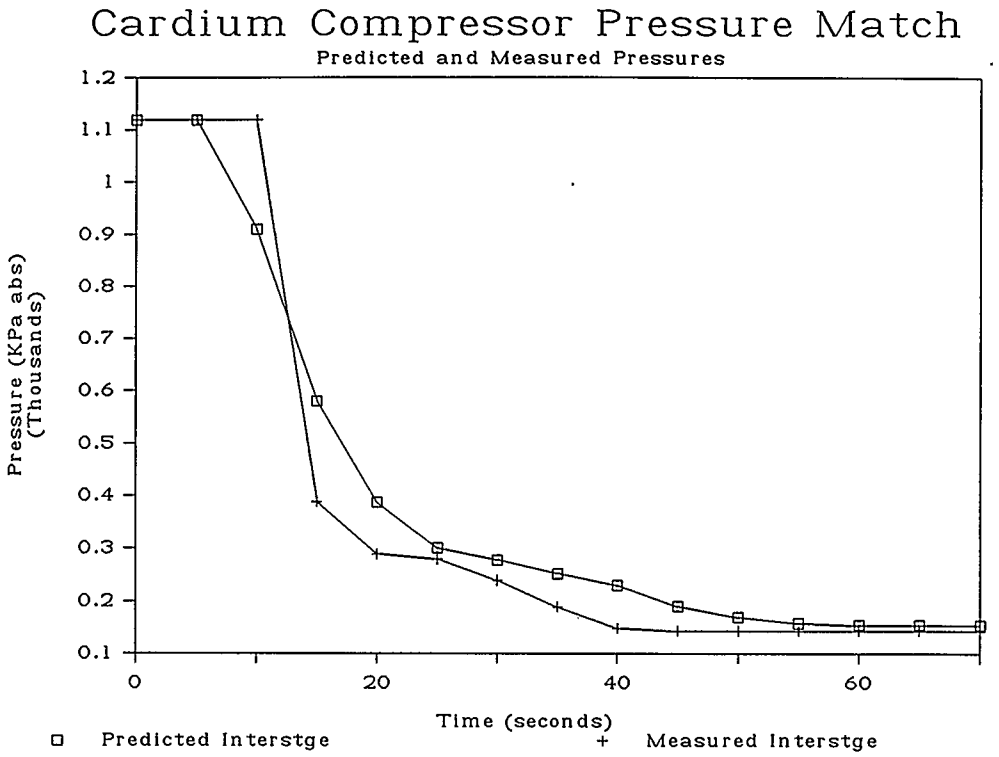

FIGURE 6.4b

Figure 6.4b shows the measured interstage pressure compared to the predicted interstage pressure. The predicted interstage pressure begins to decrease before the measured interstage pressure because of the earlier predicted time of equalization. Also, the predicted and measured data would have shown a closer match if more data points had been recorded. However, the manual recording of data for the rapid depressuring meant that readings could only be taken every five seconds.

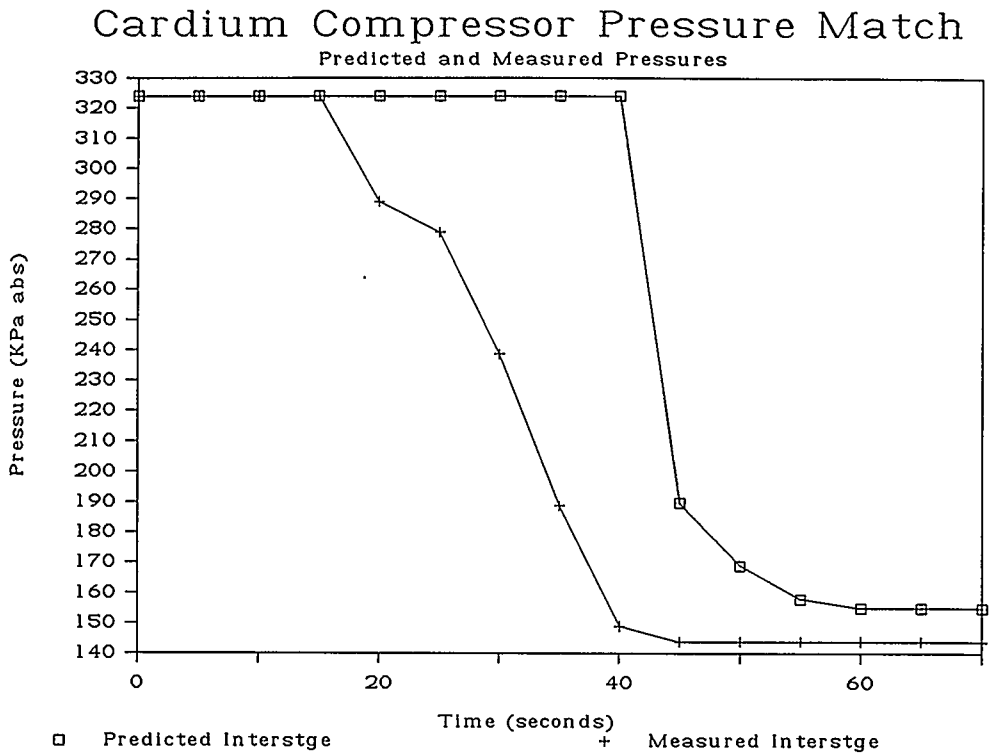

FIGURE 6.4c

Figure 6.4c shows the measured suction pressure compared to the predicted suction pressure. The predicted suction pressure equalization occurs much later than the measured pressure equalization. This is caused by a slower rate of decline of the pressure in the interstage piping. The slower rate of pressure decline may be due to a larger calculated piping volume than actually exists or flow restrictions within the compressor.

The predicted depressuring time was 60 seconds compared to an actual depressuring time of 40 seconds. The peak flare

flowrate was 114.96 $10^3 m^3_{sc}$/day at a maximum flare header pressure of 324.8 kPa abs. The comparison of the flare predictions to measured results is presented in section 6.1.10.

Comparison of Cardium to Reinjection #2 Depressuring

Both of the compressors studied exhibited the same three rate depressuring sequence. The model was able to match all three rates effectively for both compressors. The time predicted for depressuring was conservative in both cases. The Cardium Compressor depressured sooner because of the smaller piping volumes and the higher relative flare rate. The measured peak initial depressuring rate for Reinjection #2 was 7,500 kPa/min and for the Cardium Compressor was 6,000 kPa/min.

6.1.5 Recycle Valve Fail Open Prediction

The effect of failing the recycle valve open was investigated for the Reinjection Compressor #2. The predicted pressures are shown in Figure 6.5. The pressure in the suction piping increases rapidly to a maximum of 12.0 MPa abs.

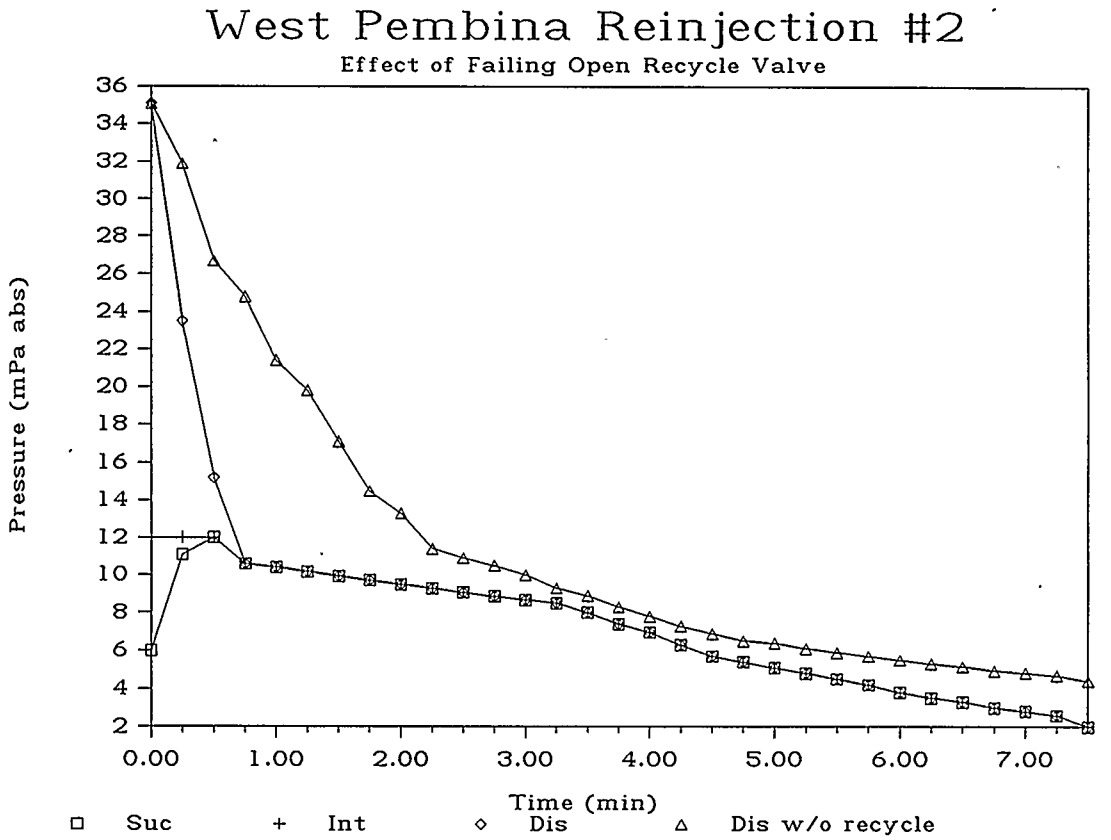

FIGURE 6.5

If the PSV were sized to handle a maximum recycle flowrate

of 1110.05 $10^3 m^3_{sc}$/day then the peak in Figure 6.5 would reach a maximum of 10,500 kPa abs. This effect is confirmed by actual experiences with Reinjection #1. The recycle valve on Reinjection #1 was originally designed to fail open. Until this was rectified the pressure in the suction piping would rise rapidly to a pressure close to the setpoint of the PSV.

The addition of a suction flare valve would decrease the risk of overpressuring, however there is the added risk of drawing air from the flare stack with a suction flare valve. The effect of installing a flare valve on the suction will be presented in section 6.1.8.

6.1.6 Temperature Profiles

The discharge and flare temperature profiles are shown in Figure 6.6a and 6.6b.

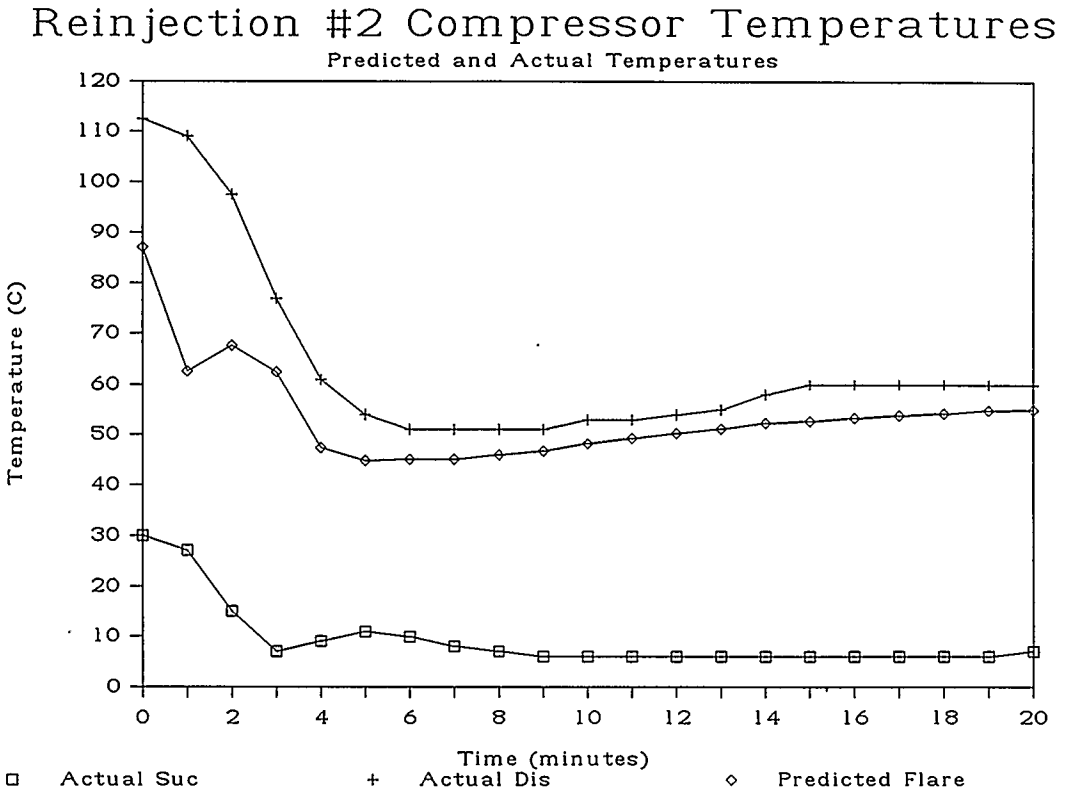

FIGURE 6.6a

The discharge temperatures were only available to be recorded for Reinjection Compressor #2. Because the West Pembina plant is on computer control, a record of the temperature as a function of time is easily available. The flare header temperature downstream of the flare valve was predicted for Reinjection Compressor #2.

The rapid decrease in discharge temperature in Figure 6.6a demonstrates that the system does not depressure in an isothermal fashion.

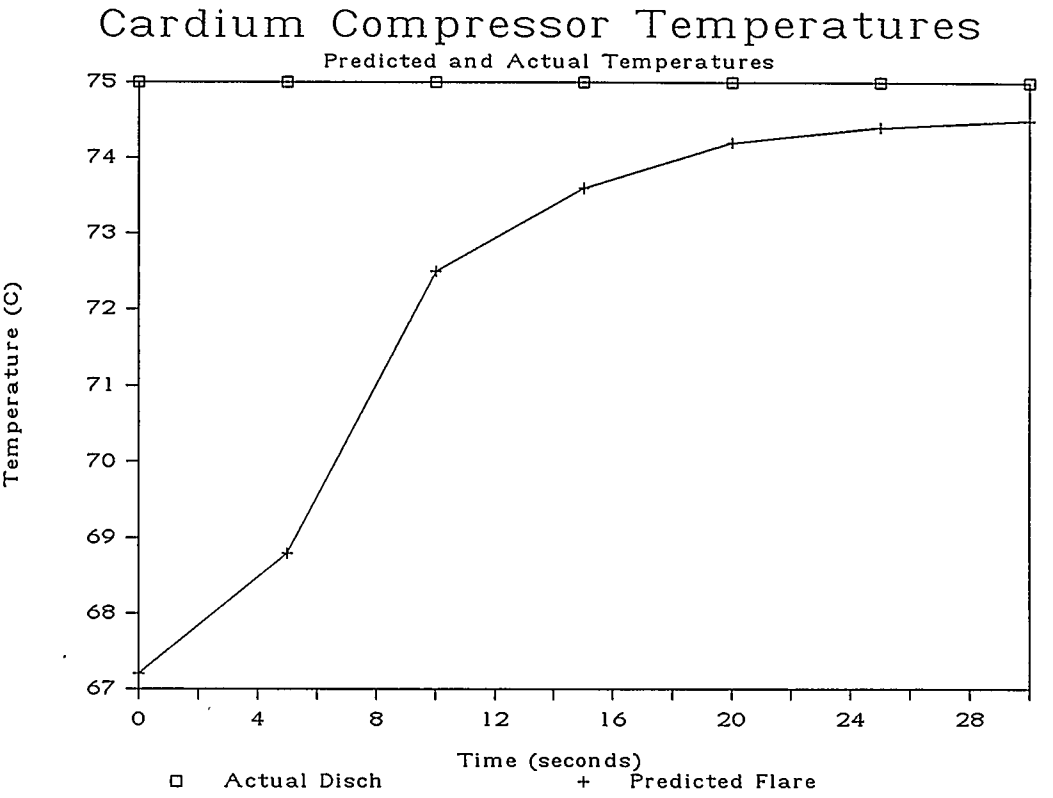

FIGURE 6.6b

Instrumentation was not available to automatically record the discharge temperature for the Cardium compressor, therefore a constant discharge temperature was assumed as shown in Figure 6.6b. This is a reasonable assumption because the effect of temperature on the pressure transient prediction was shown to be minimal in section 6.1.9.

The flare header temperature downstream of the flare valve was predicted for the Cardium Compressor. A valid temperature prediction is important to allow the design engineer to select the correct materials for the flare line. The actual flare line temperature was not available for either system to validate the flare temperature prediction, however the isenthalpic temperature drop was validated in section 6.3.

6.1.7 Effect of Installing a Suction Flare Valve on Depressuring Reinjection Compressor #2

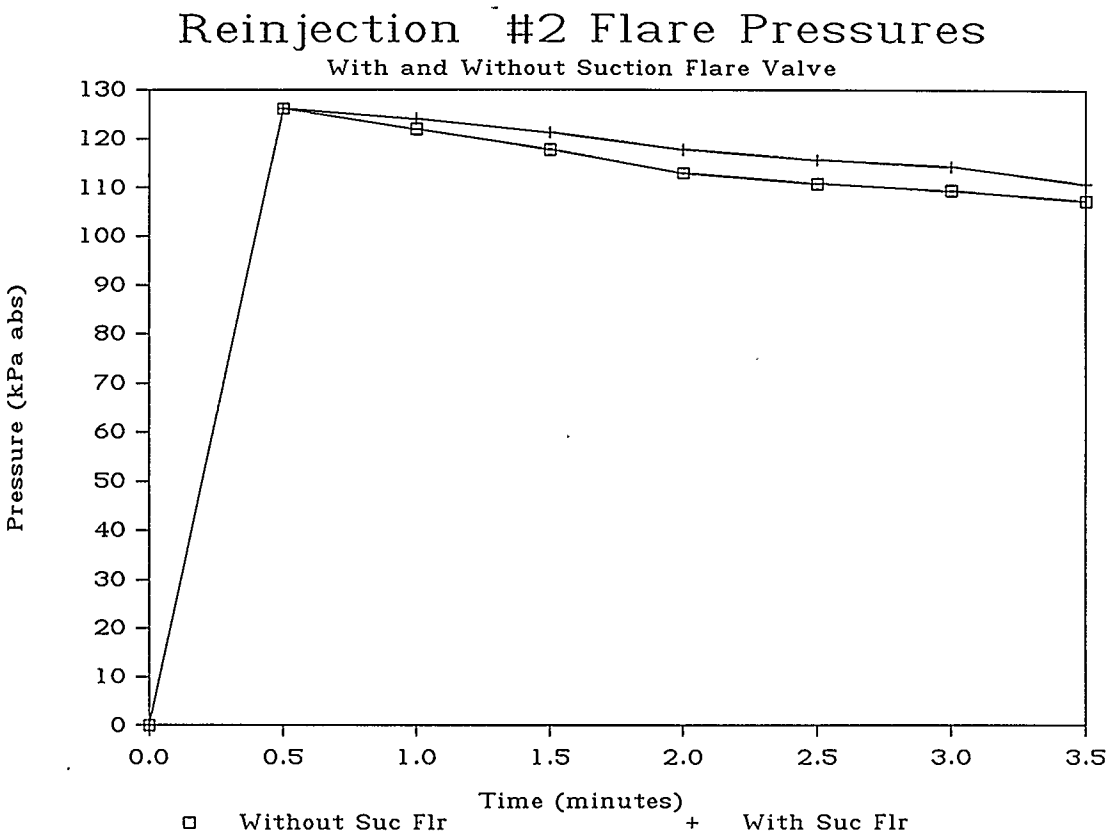

FIGURE 6.7

The effect of installing a flare valve in the suction piping is demonstrated in Figure 6.7. The suction flare valve decreases total depressuring time from 25 to 14 minutes. The total flare flowrate is increased by 9.5% from 309.9 $10^3m^3_{sc}$/day to 339.3 $10^3m^3_{sc}$/day. The peak flare header pressure was 126.2 kPa abs with or without the suction flare

valve. The reason the peak flare header pressure was unaffected is due to the small incremental flare volume and the large diameter flare line for the West Pembina main flare header.

6.1.8 Effect of Installing a Suction Flare Valve on the Flare Flowrate For Reinjection Compressor #2

The flare flowrate prediction for Reinjection #2 is shown in Figure 6.8.

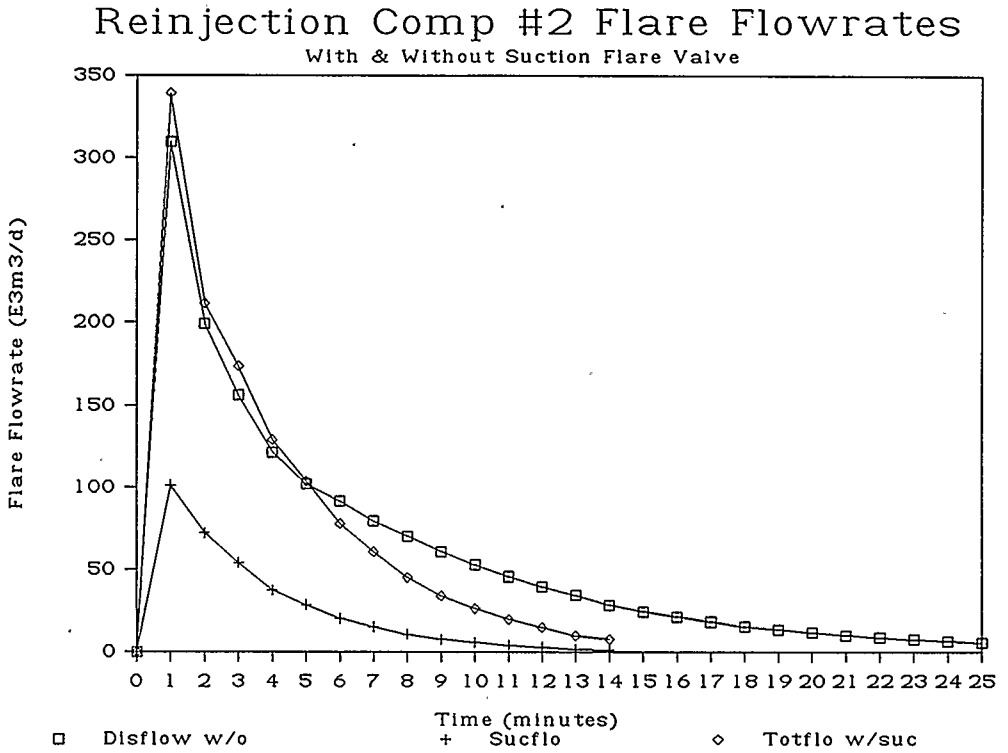

FIGURE 6.8

Figure 6.8 demonstrates the effect on the total flare flowrate of installing a flare valve in the suction piping. Figure 6.8 shows the data for the discharge flare flowrate without a suction flare valve (Disflow w/o), the suction flare flowrate (sucflo), and the total flare flowrate with a suction flare valve (Totflo w/suc). The total peak flare flowrate with a suction flare valve only slightly exceeds

the normal flare flowrate without a suction flare valve. There would only be a minimal added cost to design the flare system for the incremental flare flowrates with a suction flare valve. The cost of this valve would depend on the suction pressure, design pressure and the size of the valve.

The total area under the total flare flowrate curves should be equal for both cases, with and without the suction flare valve. A simple calculation of area demonstrates that the area under the curve with a suction flare valve is slightly less than without a suction flare valve.

6.1.9 Effect of Discharge Temperature on the Pressure Match for Reinjection Compressor #2

At an earlier stage in the model development the effect of the discharge temperature profile was investigated. The measured temperature profile was used in the model and the results are shown in Figure 6.9. The effect of incorporating measured temperature data had little impact on the ability of the model to predict the discharge pressure.

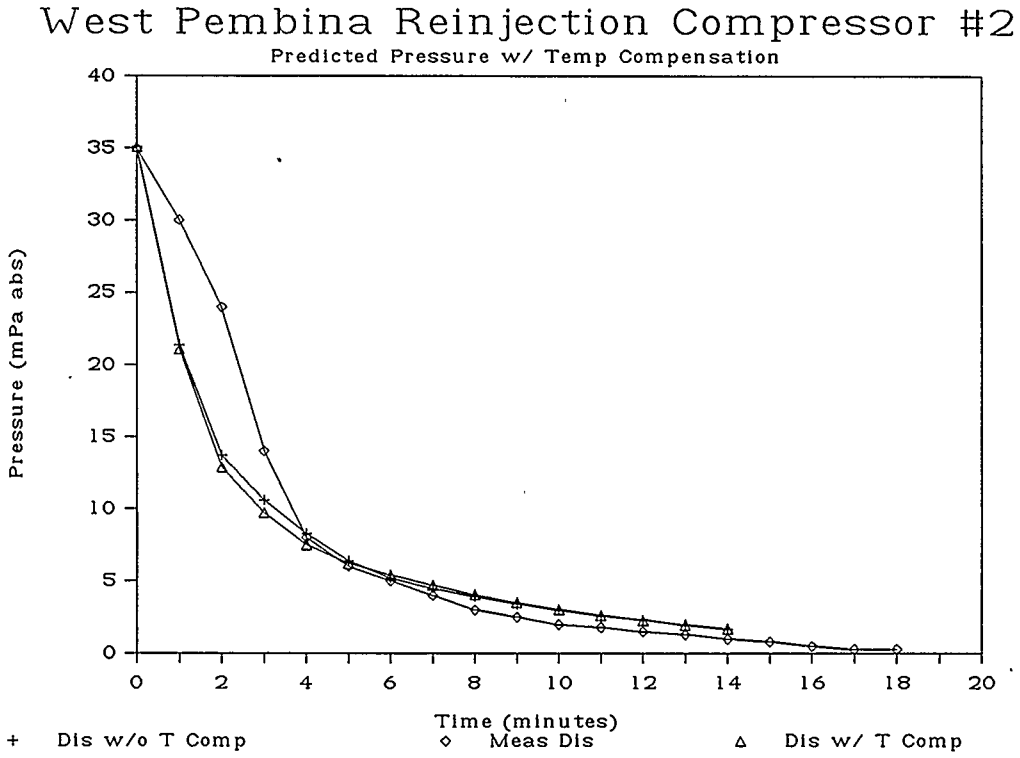

FIGURE 6.9

The greatest benefit to predicting a better temperature profile would be to facilitate a closer prediction of the

flare header temperature. The prediction of discharge piping temperature is difficult to model because of the complexities involved in integrating heat loss through an aerial cooler due to natural convection; and the prediction of temperature drop in a pipe when it is being depressured.

6.1.10 Cardium Flare System Pressure Match

Figure 6.10 shows the predicted and measured flare header pressure at the flare knockout drum. During the test the oil battery was left operating while the compressors were blocked and depressured. This meant that all the gas from the inlet separator was being flared while the test was being conducted.

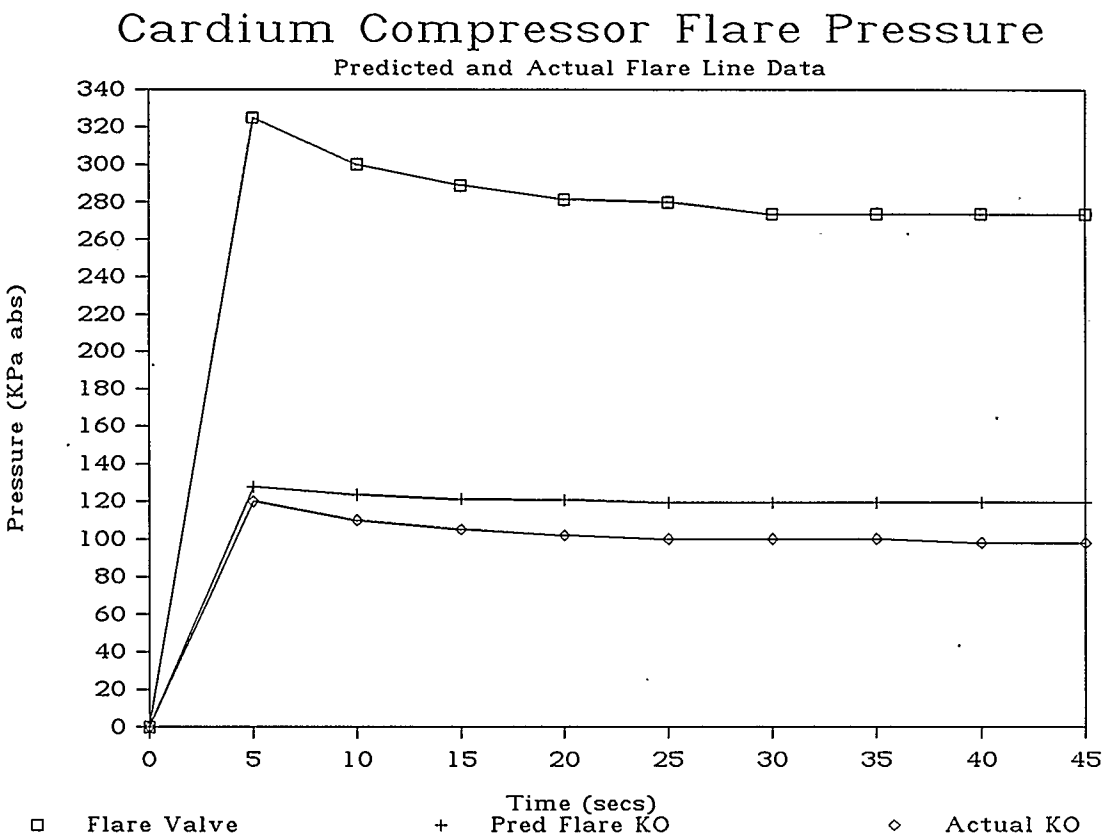

FIGURE 6.10

The pressure in the flare knockout drum is affected by the

additional 169.5 $10^3 m^3_{sc}$/day of gas being flared in the flare system from the battery. This additional flare volume was added to the flare flowrate in the program to achieve a better pressure match. During a normal block and depressure the inlet flow to the battery is shut in and the only source of flare gas is from the depressuring of the compressors. This means that during a normal depressuring the flare header pressure will be less than that shown in Figure 6.10.

6.1.11 Simplified Method to Calculate Pressure Transients

In section 4.1.7, equation 4.38 was developed to predict the depressuring time for a volume of gas, assuming an ideal gas and an isothermal process. This equation is applied to the entire piping system to make a simplified prediction of the pressure transients during the depressuring process.

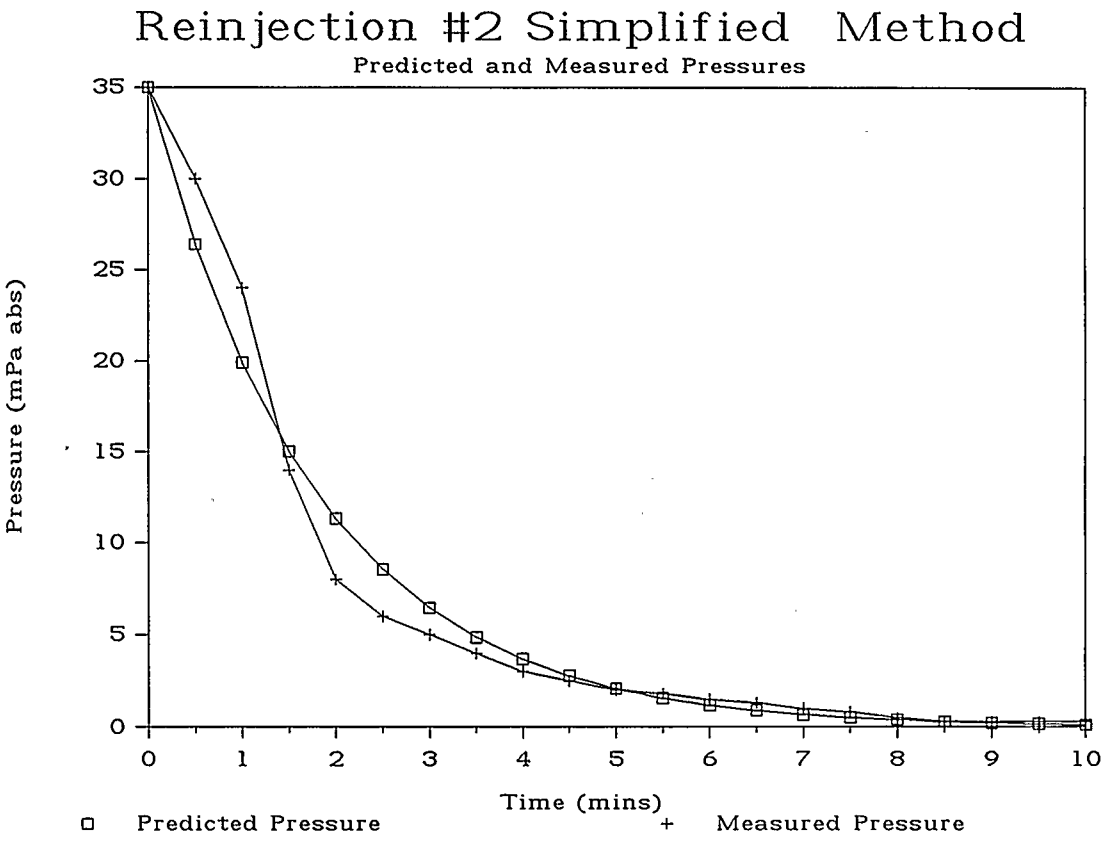

FIGURE 6.11

The simplified method has to be applied in three stages.

The first stage involves calculating the time required to depressure the discharge piping to interstage piping pressure. Stage two involves calculating the time required from the interstage pressure equalization to the time at which the interstage pressure equals the suction pressure. Stage three involves calculating the time required from suction pressure equalization to the arbitrary final end pressure.

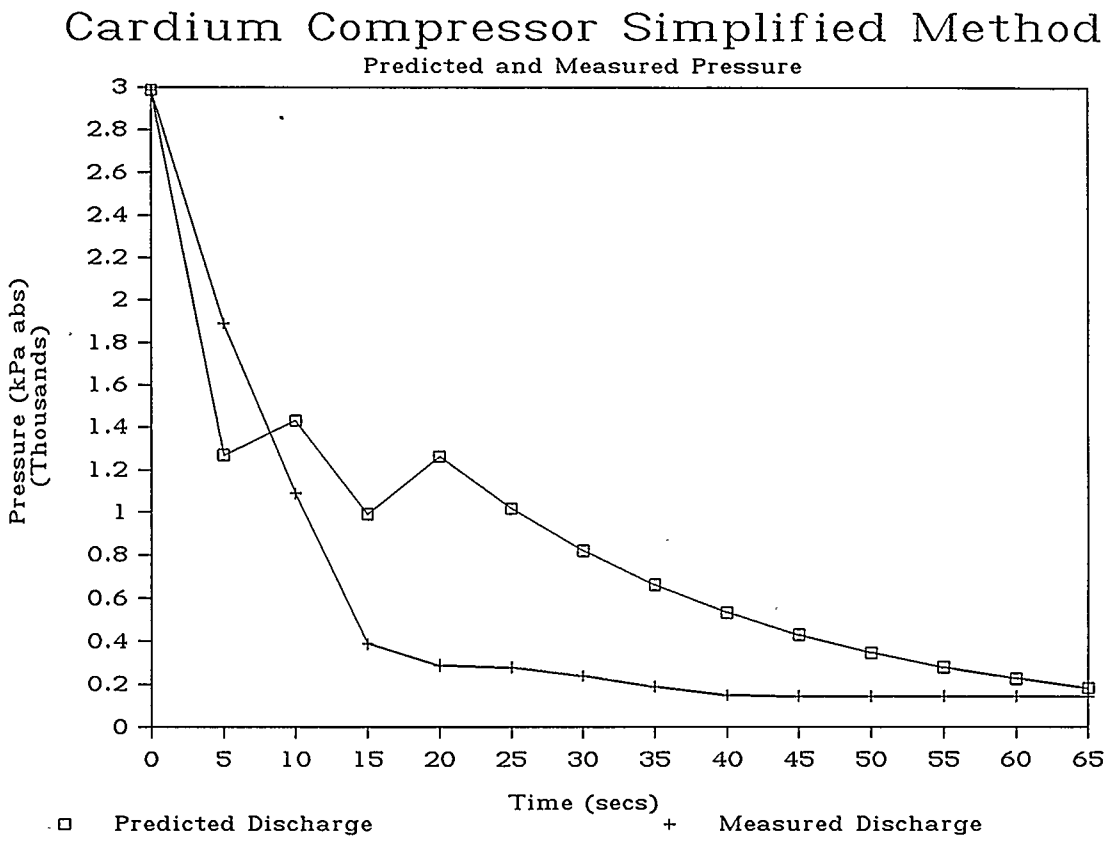

FIGURE 6.12

In Figures 6.11 and 6.12 it can be seen that the simplified method provides an adequate prediction of the depressuring pressure profile.

There are two disadvantages to the simplified approach. The calculations cannot simulate the dynamic effect of opening the recycle valve and cannot take into account the effect of valve opening time on the compressor stopping time. In addition the pressure and temperature of the flare system needs to be predicted and is not integrated into the solution.

6.2 COMPRESSOR RUNDOWN TIME AND VALVE TRAVEL TIME

The method to calculate compressor rundown time and valve travel time was developed in sections 4.4 and 4.7 respectively. In Table 6.2.1 the predicted results are compared to the recorded data.

TABLE 6.2.1 Compressor Rundown Time Summary

	Reinjection #2 Rundown Time (secs)	Cardium Rundown Time (secs)
Measured *	6.20	1.30
Predicted	7.35	1.40

* Note: measured with a stopwatch; accuracy within + or - 0.2 secs.

In Tables 6.2.2 and 6.2.3 the prediction of cylinder pressure as a function of crank angle is compared to the value calculated by Cooper[10].

TABLE 6.2.2 Compressor Rundown Pressure Prediction Compared to Cooper Data for Stage 1 Reinjection Compressor #2

Crank Angle (deg)	Head End Cooper (kPa abs)	Pressure Predicted (kPa abs)	Crank End Cooper (kPa abs)	Pressure Predicted (kPa abs)
15	9818.6	9772.4	4318.6	4318.6
30	7419.3	7220.7	4602.1	4565.5
45	5357.2	4986.2	5117.2	5027.6
60	3977.9	4227.6	5940.0	5772.4
75	3943.4	4227.6	7197.9	6931.0
90	3952.4	4227.6	9103.4	8455.2
105	3996.6	4227.6	11322.8	11041.4
120	4060.7	4227.6	11244.8	11041.4
135	4126.2	4227.6	11164.8	11041.4
150	4180.7	4227.6	11098.6	11041.4
165	4215.9	4227.6	11055.9	11041.4
180	4227.6	4227.6	11041.4	11041.4
195	4226.2	4303.4	10223.4	9689.7
210	4475.9	4565.5	8393.1	7027.6
225	4817.9	5013.8	6513.1	4772.4
240	5366.9	5751.7	5015.2	4227.6
255	6216.6	6841.4	4068.3	4227.6
270	7529.7	8641.4	4037.2	4227.6
285	9593.8	11041.4	4031.0	4227.6
300	11481.4	11041.4	4055.2	4227.6
315	11357.2	11041.4	4103.4	4227.6
330	11208.3	11041.4	4162.1	4227.6
345	11087.6	11041.4	4209.7	4227.6
360	11041.4	11041.4	4227.6	4227.6

TABLE 6.2.3 Compressor Rundown Pressure Prediction Compared to Cooper Data for Stage 2 Reinjection Compressor #2

Crank Angle (deg)	Head End Pressure Cooper (kPa abs)	Head End Pressure Predicted (kPa abs)	Crank End Pressure Cooper (kPa abs)	Crank End Pressure Predicted (kPa abs)
15	28374.5	29710.3	11566.2	11124.1
30	18776.6	21000.0	12915.9	11758.6
45	11839.3	13931.0	15208.3	12931.0
60	9595.9	10924.1	18881.4	14765.5
75	9413.8	10924.1	24700.7	15531.0
90	9460.7	10924.1	33993.1	21917.2
105	9695.9	10924.1	35030.3	28572.4
120	10033.8	10924.1	34828.3	34296.6
135	10382.8	10924.1	34619.3	34296.6
150	10671.0	10924.1	34446.2	34296.6
165	10857.2	10924.1	34334.5	34296.6
180	10934.5	10924.1	34296.6	34296.6
195	11471.0	11131.0	30929.7	30786.2
210	12511.7	11800.0	24337.9	23434.5
225	14211.7	13020.7	17809.0	16655.2
240	16893.1	14986.2	12790.3	11848.3
255	21157.2	18055.2	10470.3	10924.1
270	28155.2	22841.4	10384.1	10924.1
285	40182.8	30462.1	10366.9	10924.1
300	36458.6	34296.6	10433.8	10924.1
315	35846.9	34296.6	10571.0	10924.1
330	35115.9	34296.6	10735.9	10924.1
345	34523.4	34296.6	10849.0	10924.1
360	34296.6	34296.6	10920.7	10924.1

The measured and predicted valve travel times are shown in Tables 6.2.4 and 6.2.5. The predicted values match the measured values except for the flare valve on Reinjection Compressor #2. This may be the result of using the wrong characteristic valve flow parameter (Cg) for the solonoid on the actuator.

TABLE 6.2.4 Cardium Compressor

Valve Travel Time (secs)

	Suction	Discharge	Flare
Measured	n/a	10	2
Predicted	10.3	10.3	1.8

TABLE 6.2.5 Reinjection Compressor #2

Valve Travel Time (secs)

	Suction	Discharge	Flare
Measured	6.5	5.8	5.2
Predicted	7.6	7.9	2.8

6.3 THERMODYNAMIC PROPERTY PACKAGE VERIFICATION

The thermodynamic property package was developed in section 5 using the Lee Kesler correlations. The results of the package for each of the normal flowing conditions compared in Table 6.3.1. Hysim is an interactive thermodynamic simulator designed for the prediction of hydrocarbon and chemical process design[11].

Table 6.3.1
Comparison of Thermodynamic Predictions to Hysim*

HEAT CAPACITY
(kJ/kMOL-K)

	Flare	Suction	Interstage	Discharge
HYSIM	36.0	48.7	56.7	54.2
Predicted	34.7	46.7	55.6	53.1
ERROR	3.7%	4.2%	1.9%	2.0%

ENTHALPY
(kJ/kMOL)

	Flare	Suction	Interstage	Discharge
HYSIM	8645	8466	8285	12081
Predicted	8730	8544	8307	12077
ERROR	-0.98%	-0.93%	-0.26%	0.04%

* using the Grayson Streets/ Lee Kesler correlation.

Table 6.3.1 Continued
ZFACTOR

	Flare	Suction	Interstage	Discharge
HYSIM	0.9968	0.8442	0.8223	1.0365
Predicted	0.9969	0.8690	0.8216	1.0605
ERROR	-0.0%	-2.9%	0.1%	-2.3%

VISCOSITY
(cP)

	Flare	Suction	Interstage	Discharge
HYSIM	0.0098	0.0126	0.0174	0.0244
Predicted	0.0092	0.0125	0.0109	0.0137
ERROR	6.1%	0.8%	37.4%	43.9%

NOTE:VISCOSITY CORRELATION NOT CORRECTED FOR PRESSURE

TABLE 6.3.2
Comparison of Calculations to Lee Kesler Tabulated Values

	Tr	Pr
Flare	1.2967	0.0020
Suction	1.4659	1.5540
Interstage	1.5787	3.3683
Discharge	2.0297	7.6553

Compressibility Factors

	Predicted*		Lee Kesler	
	$Z^{(0)}$	$Z^{(1)}$	$Z^{(0)}$	$Z^{(1)}$
Flare	0.9970	0.0012	0.9985	0.0006
Suction	0.8511	0.1442	0.8477	0.1409
Interstage	0.8264	0.2531	0.8310	0.2381
Discharge	1.0601	0.3147	1.0556	0.3100

Enthalpy Factors

	Predicted*		Lee Kesler	
	$H^{(0)}$	$H^{(1)}$	$H^{(0)}$	$H^{(1)}$
Flare	0.0124	0.0054	0.0066	0.0033
Suction	0.8486	0.0522	0.8493	0.0579
Interstage	1.5027	-0.1505	1.5018	-0.1510
Discharge	1.4200	-0.4265	1.4110	-0.4240

Heat Capacity Factors

	Predicted*		Lee Kesler	
	$Cp^{(0)}$	$Cp^{(1)}$	$Cp^{(0)}$	$Cp^{(1)}$
Flare	0.0174	0.0232	0.0090	0.0120
Suction	1.3370	0.7645	1.3607	0.7294
Interstage	2.0150	0.9949	2.0160	0.9015
Discharge	1.1019	0.9032	1.4150	1.0070

* Predicted form thermodynamics model used in this thesis.

CHAPTER 7

CONCLUSIONS

In conclusion, a model has been successfully developed to predict the system response to an emergency compressor shut down. The model accurately predicts the dynamic pressure transients during a compressor shut down. Simplified methods can be accurate for simple configurations but do not facilitate the analysis of a complex system.

The complexity of the system is increased when the action of the recycle valve is changed or when a suction flare valve is installed. The effect of the action of the recycle valve was investigated and successfully incorporated into the model. The installation of the suction flare valve was modeled and the results indicate that the suction flare valve accelerated the depressuring. However, there is still the risk of drawing in air from the flare stack through the suction flare valve.

The depressuring time was predicted to be longer than the measured depressuring time for both compressors.

The predicted time for the compressor to stop rotating matched the measured data. The compressor stop time could be neglected for most studies because the time for the compressor to stop rotating is small relative to the total depressuring time.

The time to close the ESD valves was predicted accurately for the majority of valves studied. This is an area where the system designer can gain a lot of control over the depressuring sequence for very little cost.

The thermodynamic prediction used in the model yields accurate results over the range of pressures and temperatures studied. The model was successfully used to predict the heat capacity ratio (K), compressibility (Z), enthalpy(H), and viscosity for a single phase gas.

CHAPTER 8

RECOMMENDATIONS FOR FURTHER STUDY

The extension of the present dynamic model to predict the compressor discharge temperatures would facilitate a more accurate prediction of the flare header temperatures.

The model should be extended to predict the pressure and temperature transients during the depressuring sequence in other types of rotating equipment.

The use of more sophisticated integration methods should be investigated to accelerate the solution of the model. These techniques could include a predictor-corrector to accelerate convergence for each iteration. By using data from the previous iterations, the slope of the depressuring line could be estimated, and an optimized time step used to predict a new value for pressure.

REFERENCES

1. Turbo Pascal,Borland International Inc., Version 3.0, Scotts Valley California, 1986.

2. McCabe W.L. and Smith J.C., Unit Operations of Chemical Engineering, McGraw Hill, Kingsport Press Inc. USA Third Edition,1976.

3. Control Valve Handbook, Fisher Controls, Marshaltown Iowa, Second Edition, 1977.

4. Giles, R. V., 1976 Fluid Mechanics and Hydraulics, McGraw Hill, Great Britain, Second Edition, 1976.

5. Reid, R.C., Prausnitz, J. M. and Sherwood, T. K., The Properties of Gases and Liquids, McGraw Hill, Third Edition, 1977.

6. Mabie, H. H. and OcvIrk F. W., Mechanisms and Dynamics of Machinery, John Wiley and Sons, Third Edition, 1978, Blacksburg Virginnia, 1978.

7. Grote S.H.,"Calculating Pressure Release Times", Chemical Engineering, July 17, 1967, Page 203.

8. Lee, B.I. and Kesler M.G., "A Generalized Thermodynamic Correlation Based on Three Parameter Corresponding States", AICHE Journal, Vol21 No. 3 May, 1975, Page 510.

9. Engineering Data Book, Gas Processors Suppliers Association, Tenth Edition, Tulsa Oklahoma, 1987.

10. Yannes, E.J., "Engineering Study for Dome Petroleum, West Pembina Canada, Technical Report #152", Cooper Industries, Energy Services Group, Pennsylvania Process Compressors, Feb 20, 1987, Easton Pennsylvania.

11. Hysim, Hyprotech Ltd.,Version 3.33, Calgary Alberta,1988.

APPENDIX A

DATA TABLES

TABLE A.1

Reinjection # 2 Measured Depressuring Data

Time (min)	Pressure (mPa abs)		
	Suction	Interstage	Discharge
0	6.00	12.00	35.00
1	6.00	12.00	30.00
2	6.30	11.00	24.00
3	6.30	10.50	14.00
4	6.30	8.50	8.00
5	6.00	6.50	6.00
6	5.50	5.00	5.00
7	4.50	4.00	4.00
8	4.00	3.20	3.00
9	3.30	2.80	2.50
10	2.50	2.40	2.00
11	2.20	1.90	1.80
12	1.80	1.50	1.50
13	1.40	1.20	1.30
14	1.10	1.00	1.00
15	0.90	0.90	0.90
16	0.80	0.80	0.80
17	0.60	0.60	0.60
18	0.50	0.50	0.50
19	0.40	0.40	0.40
20	0.35	0.35	0.35
21	0.28	0.28	0.28
22	0.20	0.20	0.20
23	0.20	0.20	0.20
24	0.20	0.20	0.20
25	0.10	0.10	0.10

TABLE A.2
Predicted Data for Reinjection Compressor #2 from Program CM.PAS Run Date 88-04-19

Time (min)	Pressure (mPa abs)		
	Suction	Interstage	Discharge
0	6.00	12.00	35.10
1	6.22	12.00	21.70
2	6.27	12.00	13.80
3	6.33	10.27	10.27
4	6.38	7.93	7.93
5	5.83	5.83	5.83
6	5.14	5.14	5.14
7	4.51	4.51	4.51
8	3.95	3.95	3.95
9	3.46	3.46	3.46
10	3.02	3.02	3.02
11	2.64	2.64	2.64
12	2.31	2.31	2.31
13	2.01	2.01	2.01
14	1.76	1.76	1.76
15	1.53	1.53	1.53
16	1.33	1.33	1.33
17	1.16	1.16	1.16
18	0.97	0.97	0.97
19	0.84	0.84	0.84
20	0.74	0.74	0.74
21	0.67	0.67	0.67
22	0.59	0.59	0.59
23	0.51	0.51	0.51
24	0.45	0.45	0.45
25	0.39	0.39	0.39

TABLE A.3

Brazeau Cardium Measured Data 88-04-27

Time (secs)	Pressure (kPa abs)		
	Suction	Interstage	Discharge
0	324.0	1119.0	2989.0
5	389.0	1089.0	1889.0
10	324.0	1119.0	1089.0
15	324.0	389.0	389.0
20	289.0	289.0	289.0
25	279.0	279.0	279.0
30	239.0	239.0	239.0
35	189.0	189.0	189.0
40	149.0	149.0	149.0
45	144.0	144.0	144.0
50	144.0	144.0	144.0
55	144.0	144.0	144.0
60	144.0	144.0	144.0
65	144.0	144.0	144.0
70	144.0	144.0	144.0

TABLE A.4

Predicted Depressuring Data

for the Cardium Compressor

From Program cmc.pas 88-04-30

Time (secs)	Pressure (kPa abs)		
	Suction	Interstage	Discharge
0	324.0	1119.0	2989.0
5	324.0	1119.0	1907.0
10	324.0	911.0	911.0
15	324.0	581.0	581.0
20	324.0	388.0	388.0
25	324.0	301.0	301.0
30	324.0	278.0	278.0
35	324.0	252.0	252.0
40	324.0	230.0	230.0
45	190.0	190.0	190.0
50	169.0	169.0	169.0
55	158.0	158.0	158.0
60	155.0	155.0	155.0
65	155.0	155.0	155.0
70	155.0	155.0	155.0

TABLE A.5
Predicted Pressures for Reinjection Compressor #2
from Programs CMR.PAS 88-05-18 and from CM.PAS 88-05-17
RECYCLE VALVE FAIL OPEN

Time (min)	Pressure (mPa abs)				
	Suction With Recycle Valve	Interstage	Discharge	Discharge w/o Rec	Rec Flow ($10^3 m^3_{sc}/d$)
0.00	6.00	12.00	35.10	35.10	1110.5
0.25	11.10	12.00	23.50	31.90	567.2
0.50	12.00	12.00	15.20	26.70	
0.75	10.60	10.60	10.60	24.80	
1.00	10.40	10.40	10.40	21.40	
1.25	10.17	10.17	10.17	19.80	
1.50	9.93	9.93	9.93	17.10	
1.75	9.71	9.71	9.71	14.50	
2.00	9.49	9.49	9.49	13.30	
2.25	9.27	9.27	9.27	11.40	
2.50	9.06	9.06	9.06	10.90	
2.75	8.85	8.85	8.85	10.50	
3.00	8.66	8.66	8.66	10.00	
3.25	8.50	8.50	8.50	9.30	
3.50	8.00	8.00	8.00	8.90	
3.75	7.40	7.40	7.40	8.30	
4.00	6.96	6.96	6.96	7.80	
4.25	6.30	6.30	6.30	7.30	
4.50	5.70	5.70	5.70	6.89	
4.75	5.40	5.40	5.40	6.50	
5.00	5.10	5.10	5.10	6.39	
5.25	4.80	4.80	4.80	6.10	
5.50	4.50	4.50	4.50	5.90	
5.75	4.20	4.20	4.20	5.70	
6.00	3.80	3.80	3.80	5.50	
6.25	3.50	3.50	3.50	5.30	
6.50	3.30	3.30	3.30	5.16	
6.75	3.00	3.00	3.00	4.95	
7.00	2.80	2.80	2.80	4.82	
7.25	2.60	2.60	2.60	4.70	
7.50	2.00	2.00	2.00	4.40	

TABLE A.6a

Reinjection #2 Temperature Profile

Time (min)	Actual Suction (C)	Actual Discharge (C)	Predicted Flare (C)
0	30.0	112.5	87.1
1	27.0	109.0	62.6
2	15.0	97.5	67.7
3	7.0	77.0	62.4
4	9.0	61.0	47.3
5	11.0	54.0	44.8
6	10.0	51.0	45.1
7	8.0	51.0	45.0
8	7.0	51.0	46.0
9	6.0	51.0	46.7
10	6.0	53.0	48.2
11	6.0	53.0	49.3
12	6.0	54.0	50.3
13	6.0	55.0	51.2
14	6.0	58.0	52.4
15	6.0	60.0	52.7
16	6.0	60.0	53.3
17	6.0	60.0	53.8
18	6.0	60.0	54.2
19	6.0	60.0	54.9
20	7.0	60.0	55.0

TABLE A.6b

Cardium Compressor Temperature Profiles

Time (min)	Discharge Temperature (C)	Predicted Flare (C)
0	75.0	67.2
5	75.0	68.8
10	75.0	72.5
15	75.0	73.6
20	75.0	74.2
25	75.0	74.4
30	75.0	74.5

TABLE A.7

Predicted Flare Header Pressure

With and Without Suction Flare Valve

Reinjection Compressor #2

Time (mins)	Flare Pressure w/o suc flr vlv (kPa abs)	Flare Pressure W/ suc flr vlv (kPa abs)
0.0	0.0	0.0
0.5	126.2	126.2
2.0	122.1	124.1
2.5	118.4	121.4
2.0	114.8	117.9
2.5	111.0	115.9
3.0	109.7	114.5
3.5	107.6	111.0

Table A.8
Reinjection # 2 Compressor
Flare Flowrates With and Without Suction Flare Valve

Time (min)	W/o Sucflr vlv Flare ($10^3 m^3_{sc}/d$)	Suc Flare ($10^3 m^3_{sc}/d$)	W/Suc Flr Valv Total Flare ($10^3 m^3_{sc}/d$)
0	0.0	0.0	0.0
1	309.87	101.19	339.30
2	199.36	7708	211.75
3	156.23	54.06	173.74
4	121.36	37.60	128.92
5	102.02	28.76	103.74
6	91.35	20.41	77.82
7	79.48	15.25	60.76
8	70.11	10.79	45.18
9	60.91	7.84	34.26
10	52.88	5.82	26.53
11	45.88	4.12	19.85
12	39.76	2.96	15.10
13	34.55	1.73	10.09
14	28.48	1.09	7.95
15	24.65		
16	21.35		
17	18.46		
18	15.58		
19	13.81		
20	11.93		
21	10.30		
22	8.89		
23	7.67		
24	6.62		
25	5.69		

TABLE A.9

Discharge Temperature Compensation

Reinjection Compressor #2

Predicted Pressures from CM.PAS 88-04-19

Time (min)	Pressure (mPa abs)			
	Suction	Interstage	Discharge	Disch With Temp Comp
0	6.0	12.0	35.1	35.1
1	6.5	12.0	21.4	21.1
2	6.6	12.0	13.7	12.9
3	6.8	10.6	10.6	9.7
4	6.9	8.3	8.3	7.5
5	6.4	6.4	6.4	6.2
6	5.2	5.2	5.2	5.4
7	4.5	4.5	4.5	4.7
8	3.9	3.9	3.9	4.1
9	3.4	3.4	3.4	3.5
10	3.0	3.0	3.0	3.0
11	2.6	2.6	2.6	2.6
12	2.3	2.3	2.3	2.3
13	1.9	1.9	1.9	2.0
14	1.7	1.7	1.7	1.7

TABLE A.10

Cardium Compressor Flare System Pressure Prediction

	Predicted		Measured
Time (secs)	Flare Valve (kPa abs)	Flare Knockout (kPa abs)	Flare Knockout (kPa abs)
0	0.0	0.0	0.0
5	324.8	127.6	120.0
10	300.0	123.4	110.0
15	289.0	121.4	105.0
20	281.4	120.7	102.0
25	280.0	119.3	100.0
30	273.8	119.3	100.0
35	273.8	119.3	100.0
40	273.8	119.3	98.0
45	273.8	119.3	98.0

TABLE A.11
Reinjection Compressor #2 Simplified Method

Time (min)	Predicted Pressure (mPa abs)	Measured Pressure (mPa abs)
0	35.0	35.0
1	19.9	30.0
2	11.3	24.0
3	5.5	14.0
4	4.2	8.0
5	5.5	6.0
6	4.7	5.0
7	4.0	4.0
8	3.4	3.0
9	2.9	2.5
10	2.5	2.0
11	2.1	1.8
12	1.8	1.5
13	1.5	1.3
14	1.3	1.0
15	1.1	0.8
16	0.9	0.5
17	0.8	0.3
18	0.7	0.3
19	0.6	0.3
20	0.5	0.3

TABLE A.12
Cardium Compressor Simplified Method

Time (secs)	Predicted Pressure (kPa abs)	Measured Pressure (kPa abs)
0	2989.0	2989.0
5	1268.6	1889.0
10	1431.1	1089.0
15	990.2	389.0
20	1263.1	289.0
25	1018.4	279.0
30	821.1	239.0
35	662.0	189.0
40	533.7	149.0
45	430.3	144.0
50	347.0	144.0
55	279.7	144.0
60	225.5	144.0
65	181.8	144.0

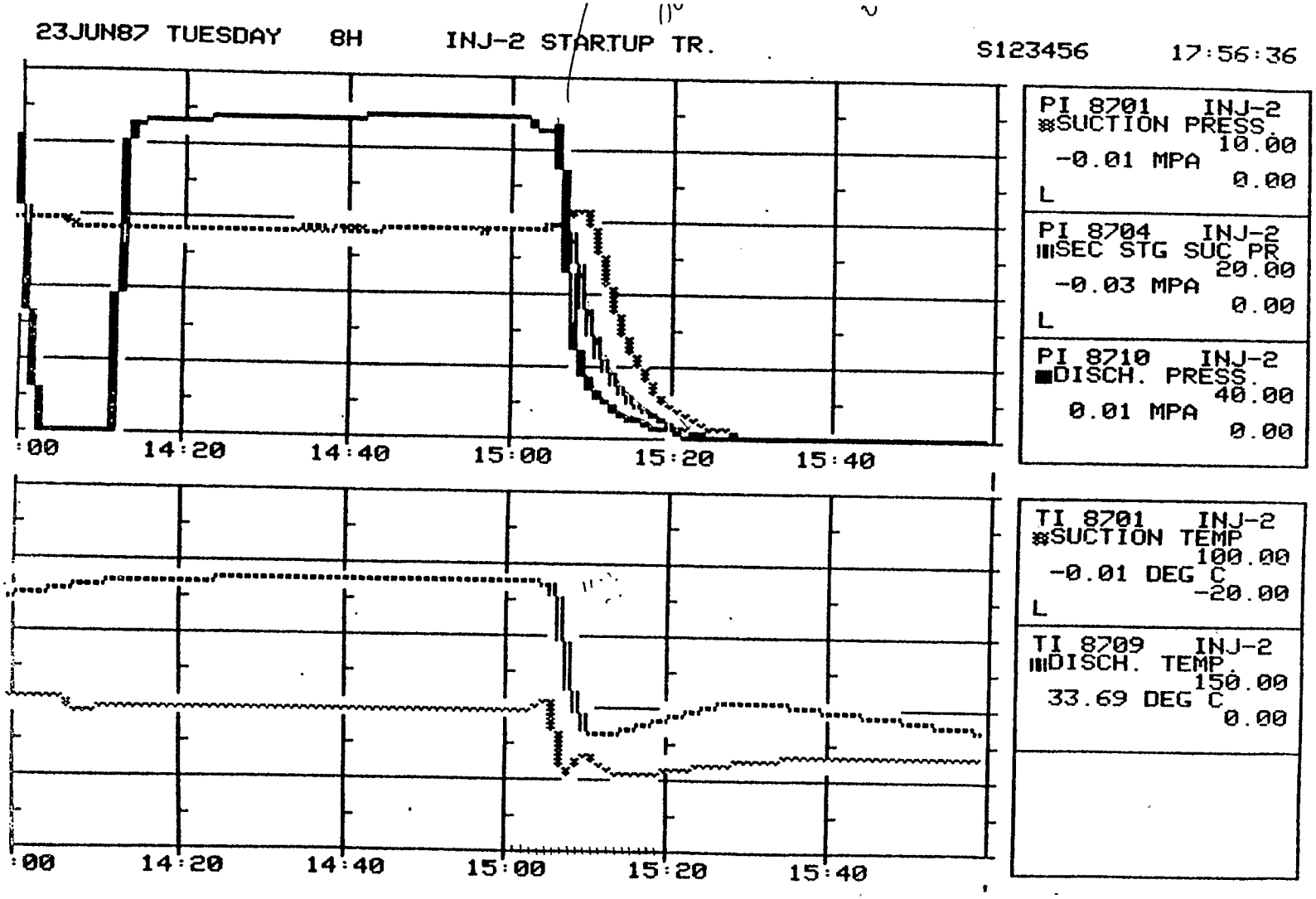
23JUN87 TUESDAY 8H
INJ-2 STARTUP TR.
S123456
17:56:36
PI 8701 INJ-2
SUCTION PRESS.
10.00
-0.01 MPA
0.00
L
PI 8704 INJ-2
SEC STG SUC PR
20.00
-0.03 MPA
0.00
L
PI 8710 INJ-2
DISCH. PRESS.
40.00
0.01 MPA
0.00
:00
14:20
14:40
15:00
15:20
15:40
TI 8701 INJ-2
SUCTION TEMP
100.00
-0.01 DEG C
-20.00
L
TI 8709 INJ-2
DISCH. TEMP
150.00
33.69 DEG C
0.00
:00
14:20
14:40
15:00
15:20
15:40

APPENDIX C

DERIVATION OF EQUATIONS

Derivation of Equation 4.1 and 4.2

The rate of evacuation of a fixed volume is governed by the law of conservation of mass:

$$\frac{\partial m}{\partial t} = \text{mass in} - \text{mass out} \qquad -(C.1)$$

Dividing by molecular weight and using a discrete time interval equation C.1 becomes:

$$\frac{\Delta n}{\Delta t} = \dot{n}_{in} - \dot{n}_{out} \qquad -(C.2)$$

where

$$\dot{n} = \frac{\partial n}{\partial t} \qquad -(C.3)$$

Equation C.2 becomes:

$$n_{t+1} = n_t - \left(\dot{n}_{in} - \dot{n}_{out}\right)\Delta t \qquad -(C.4)$$

where:

$$\Delta n = n_{t+1} - n_t \qquad -(C.5)$$